

CALCULATION OF AIRBLAST FROM UNDERGROUND  
AMMUNITION STORAGE MAGAZINES

LYNN W. KENNEDY  
KENNETH D. SCHNEIDER  
CHARLES E. NEEDHAM

15 AUGUST 1984

S-CUBED  
(A Division of Maxwell Laboratories, Inc.)  
5905 Marble Avenue, N.E.  
Albuquerque, N. M. 87110

Prepared for:  
NORWEGIAN DEFENCE CONSTRUCTION SERVICE  
Oslo mil/Akershus  
OSLO 1, Norway  
and  
DEPARTMENT OF DEFENSE  
Explosives Safety Board  
2461 Eisenhower Avenue  
Alexandria, VA 22331

# COMPONENT PART NOTICE

THIS PAPER IS A COMPONENT PART OF THE FOLLOWING COMPILATION REPORT:

TITLE: Minutes of the Explosives Safety Seminar (22nd) Held in Anaheim,  
California on 26-28 August 1986, Volume 1.

TO ORDER THE COMPLETE COMPILATION REPORT, USE AD-A181 274.

THE COMPONENT PART IS PROVIDED HERE TO ALLOW USERS ACCESS TO INDIVIDUALLY AUTHORED SECTIONS OF PROCEEDING, ANNALS, SYMPOSIA, ETC. HOWEVER, THE COMPONENT SHOULD BE CONSIDERED WITHIN THE CONTEXT OF THE OVERALL COMPILATION REPORT AND NOT AS A STAND-ALONE TECHNICAL REPORT.

THE FOLLOWING COMPONENT PART NUMBERS COMPRISE THE COMPILATION REPORT:

AD#: P005 302 thru P005 349 AD#: \_\_\_\_\_  
AD#: \_\_\_\_\_ AD#: \_\_\_\_\_  
AD#: \_\_\_\_\_ AD#: \_\_\_\_\_

Accession For	
NTIS GRA&I	<input checked="checked" type="checkbox"/>
DTIC TAB	<input type="checkbox"/>
Unannounced	<input type="checkbox"/>
Justification	
By _____	
Distribution/	
Availability Codes	
Dist	Avail and/or Special
A-1	

DTIC FORM 463  
MAR 85

This document has been approved  
for public release and sale; its  
distribution is unlimited.

OPI: DTIC-TID

## TABLE OF CONTENTS

### SECTION

I	INTRODUCTION.....	1
II	PHASE 1: DETONATION AND INTERIOR PROPAGATION.....	3
III	PHASE 2: EXPANSION INTO EXTERIOR REGION.....	28
IV	PHASE 3: ONE-DIMENSIONAL CALCULATIONS.....	36
V	PHASE 4: NONLINEAR ACOUSTIC WAVE SOLUTION (NLAWS) ..	50
VI	CONCLUSIONS.....	53

## LIST OF FIGURES

FIGURE		PAGE
1	Schematic Diagram for Norwegian Underground Storage Bunker Calculation (not to scale) .....	4
2	Pressure Contours in Explosive Chamber at 150 $\mu$ sec After Detonation .....	6
3	Energy Contours in Explosive Chamber at 150 $\mu$ sec After Detonation .....	7
4	Pressure Contours in Vertical Chamber and Passageway at 340 $\mu$ sec After Detonation..	8
5	Energy Contours in Vertical Chamber and Passageway at 340 $\mu$ sec After Detonation..	9
6	Pressure Contours in Vertical Chamber and Entrance Tunnel at 500 $\mu$ sec After Detonation .....	10
7	Energy Contours in Vertical Chamber and Entrance Tunnel at 500 $\mu$ sec After Detonation .....	11
8	Pressure Contours in Tunnel Entrance Region at 900 $\mu$ sec After Detonation .....	12
9	Energy Contours in Tunnel Entrance Region at 900 $\mu$ sec After Detonation .....	13
10	Overpressure versus Time Record at Measuring Point 1 .....	15
11	Overpressure versus Time Record at Measuring Point 2 .....	16
12	Overpressure versus Time Record at Measuring Point 3 .....	17
13	Overpressure versus Time Record at Measuring Point 4 .....	18
14	Overpressure versus Time Record at Measuring Point 5 .....	19
15	Density versus Time Record at Measuring Point 5 .....	20

# LIST OF FIGURES (Continued)

FIGURE		PAGE
16	Overpressure versus Time Record at Tunnel Entrance, Near the Floor .....	22
17	Horizontal Velocity versus Time Record at Tunnel Entrance, Near the Floor .....	23
18	Overpressure versus Time Record at Tunnel Entrance, Near the Center .....	24
19	Horizontal Velocity versus Time Record at Tunnel Entrance, Near the Center .....	25
20	Overpressure versus Time Record at Tunnel Entrance, Near the Roof .....	26
21	Horizontal Velocity versus Time Record at Tunnel Entrance, Near the Roof .....	27
22	Calculational Configuration for Phase 2 .....	29
23	Pressure Contours in Exterior Region at 1.5 msec After Detonation .....	30
24	Density Contours in Exterior Region at 1.5 msec After Detonation .....	31
25	Energy Contours in Exterior Region at 1.5 msec After Detonation .....	32
26	Pressure Contours in Exterior Region at 2.3 msec After Detonation .....	33
27	Density Contours in Exterior Region at 2.3 msec After Detonation .....	34
28	Energy Contours in Exterior Region at 2.3 msec After Detonation .....	35
29	Calculational Configuration Showing Lines Along Which One-Dimensional Calculations Were Performed .....	37

# LIST OF FIGURES (Continued)

FIGURE		PAGE
30	Pressure Contours at 3.1 msec Used for Initiation of Phase 3 .....	38
31	Energy Contours at 3.1 msec Used for Initiation of Phase 3 .....	39
32	Density Contours at 3.1 msec Used for Initiation of Phase 3 .....	40
33	Flow Velocity Vector Plot at 3.1 msec Used for Initiation of Phase 3 .....	41
34	Overpressure versus Range Plot Along 90-deg Line at 12.15 msec .....	43
35	Overpressure versus Range Plot Along 75-deg Line at 12.00 msec .....	44
36	Overpressure versus Range Plot Along 60-deg Line at 12.00 msec .....	45
37	Overpressure versus Range Plot Along 45-deg Line at 12.50 msec .....	46
38	Overpressure versus Range Plot Along 30-deg Line at 12.50 msec .....	47
39	Overpressure versus Range Plot Along 15-deg Line at 12.50 msec .....	48
40	Overpressure versus Range Plot Along 0-deg Line at 12.50 msec .....	49
41	Overpressure versus Range Plot Showing Method of Determining Triangular Wave Input for NLAWS .....	51
42	Ranges for 50 and 200 mbar Peak Overpressures as Functions of Angle .....	54

# CALCULATION OF AIRBLAST FROM UNDERGROUND AMMUNITION STORAGE MAGAZINES

## I. INTRODUCTION

The storage of munitions in underground facilities provides a potential hazard to surrounding buildings or populations. Current placement of such facilities relative to above-ground structures is based on long standing curves and scaling relations for the peak airblast overpressure as a function of weight of explosives and distance and angle relative to the tunnel opening. The suggested scaling relation for a 50 mbar safety criterion is

$$d = D \cdot F \cdot P_o^{0.67}$$

where  $d$  is the distance to 50 mbar (m)  
 $D$  is the main tunnel diameter (m)  
 $P_o$  is the gas pressure in the main passageway (bars)  
and  $F$  is a tabulated directional factor.

This relationship is based on a variety of explosive weight-to-volume ratios. However, recent storage designs call for larger amounts of explosives and lower explosive storage densities than were considered in developing the relationship. It has not been demonstrated that the same relation holds for these new conditions. In addition, the high cost of real estate suggests that small changes in the safe distances will have a significant financial impact on the storage of munitions.

A coordinated program of experiments and calculations is being conducted by the Norwegian Defence Construction

Service (NDCS) to reduce the uncertainties in determination of safe distances and to define the angular distribution of overpressure. As a part of this program, S-CUBED provided hydrodynamic flow calculations of the detonation, internal propagation and external expansion of blast waves in a two-dimensional model designed to simulate the NDCS experiment, "Test 1". The calculation was done in four consecutive phases, which are described in the next four sections. Codes used were HULL, a two or three dimensional, state-of-the-art, finite difference Eulerian hydrodynamic flow program; SAP (Spherical Air PUFF), a one-dimensional, spherically-symmetric version of HULL; and NLAWS, an acoustic wave propagation code. Using multiple phases in this way, efficiency of computer time is maximized while essential features of the result are retained. This summary report provides a description of the calculation and presents the results that were obtained.



## II. PHASE 1: DETONATION AND INTERIOR PROPAGATION

The first phase of the calculation included detonation of an explosive in an enclosed region which was designed to simulate the interior tunnel complex of the NDCS test model. Propagation of blast waves in the enclosed chambers and exit of blast pressure at the tunnel mouth were monitored from time zero (initiation of the detonation) to 4.24 msec after detonation.

The calculational configuration used for this phase is illustrated in Figure 1. The calculational mesh is a rectangular grid in two-dimensions. The HULL code was used for this phase, as well as for Phase 2. In order to simulate the three-dimensional test chamber in two dimensions, it was necessary to change the orientations of the detonation and expansion chambers. In the test configuration, the entranceway and expansion chamber are oriented so that their long axes are horizontal and perpendicular to each other. The explosive chamber axis is vertical. In the calculational configuration, the right angle orientations are retained, but all chambers lie in the same plane.

Also because the coordinate system is rectangular while some of the test chambers have circular cross sections, it was necessary to adjust the dimensions slightly in order to maintain the appropriate cross-sectional areas and chamber volumes. If the unit depth (into the paper in Figure 1) is assumed to be 5 cm, then all of the chamber cross sections and volumes are the same as for the test configuration. The total internal volume of the complex is  $17,212 \text{ cm}^3$ . Dimensions of the undetonated explosive were also adjusted so that, using the same 5-cm depth and a density of  $1.66 \text{ gms/cm}^3$ , the mass of the charge was 200 gms, corresponding to that used in the test.

Grid size for this calculation is approximately 0.5 cm vertically by 0.8 cm horizontally, although adjustments were made so that cell boundaries would coincide with the previously determined material boundaries. There are  $70 \times 376$ , or approximately 26,000, calculational cells in the grid.

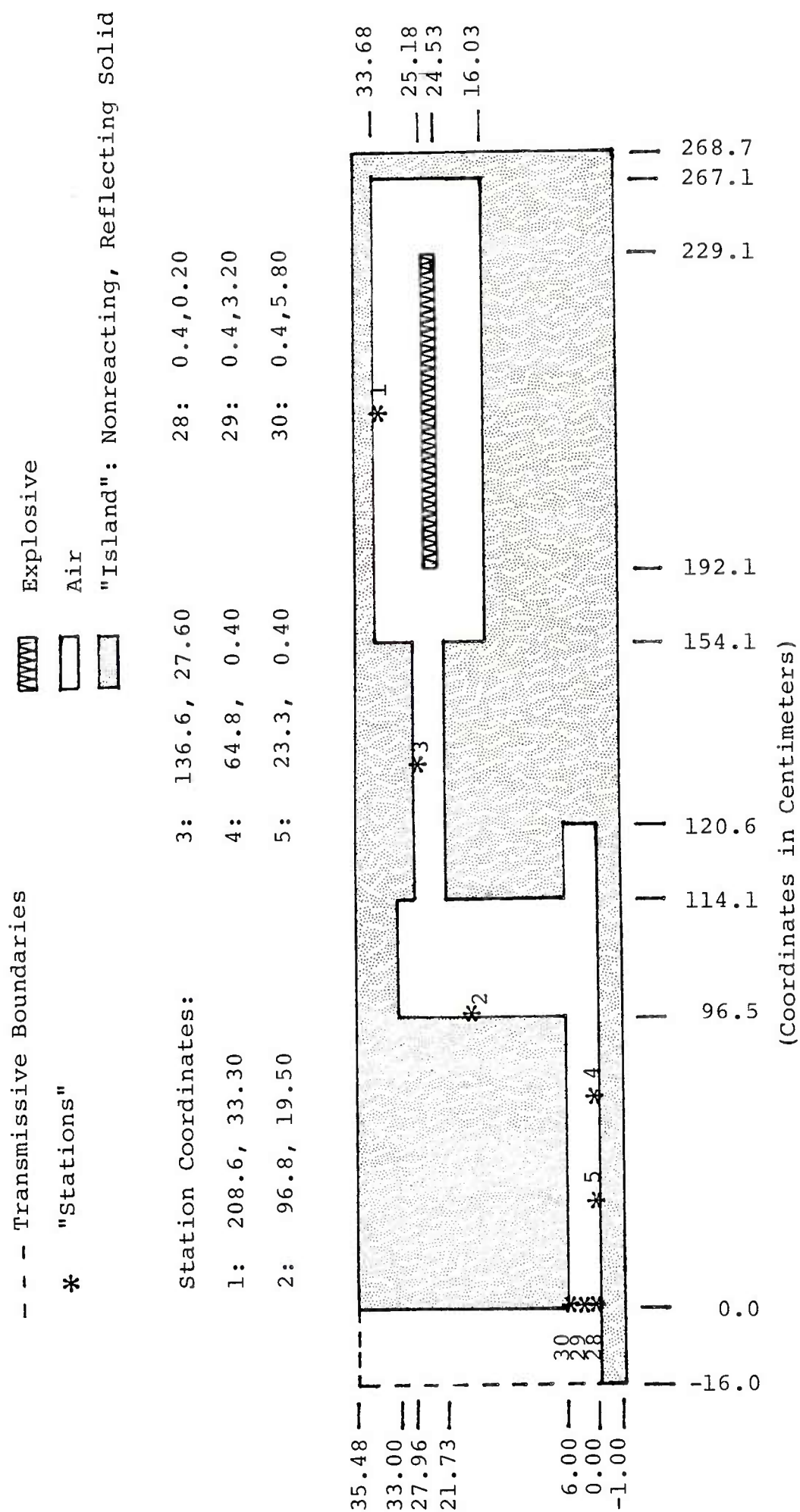


Figure 1. Schematic Diagram for Norwegian Underground Storage Bunker Calculation (not to scale)

The calculation was begun at a time set arbitrarily to 10  $\mu$ sec. At this time, the calculational zone at the right-hand edge of the explosive was considered to be detonated. The detonation wave progressed through the explosive from right to left as the calculation proceeded.

Two types of graphical output are routinely provided by HULL, and selected examples are included in this report. The first is "contour" plots, in which isograms of any of the hydrodynamic variables are shown throughout the region of interest. Figures 2 through 9 are contour plots of pressure and energy at four different times during the interior calculation. In Figures 2 and 3, at 150  $\mu$ sec, it can be seen that the explosive has detonated but the energy has not yet started to escape from the explosive chamber. Pressure and energy values throughout the chamber are very high.

In Figures 4 and 5, at 340  $\mu$ sec, a shock wave has traveled through the narrow passageway, reflected from the left-hand side of the vertical chamber, and is moving downward. Pressures are very high at the left-hand side of the vertical chamber where the flow has stagnated, and reflected shocks from the corners are visible in the explosive chamber.

The next two figures, 6 and 7, illustrate the situation of 500  $\mu$ sec. At this time, energy is moving down the long entrance tunnel. The interesting point about the flow in this region is that the energy contours are not perpendicular to the tunnel walls. Because of the right-angle bend, energies are higher near the bottom of the tunnel.

The last set of contour plots was made at 900  $\mu$ sec, and is shown in Figures 8 and 9. In this set, the shock has reached the tunnel entrance and is expanding as it moves into the exterior space.

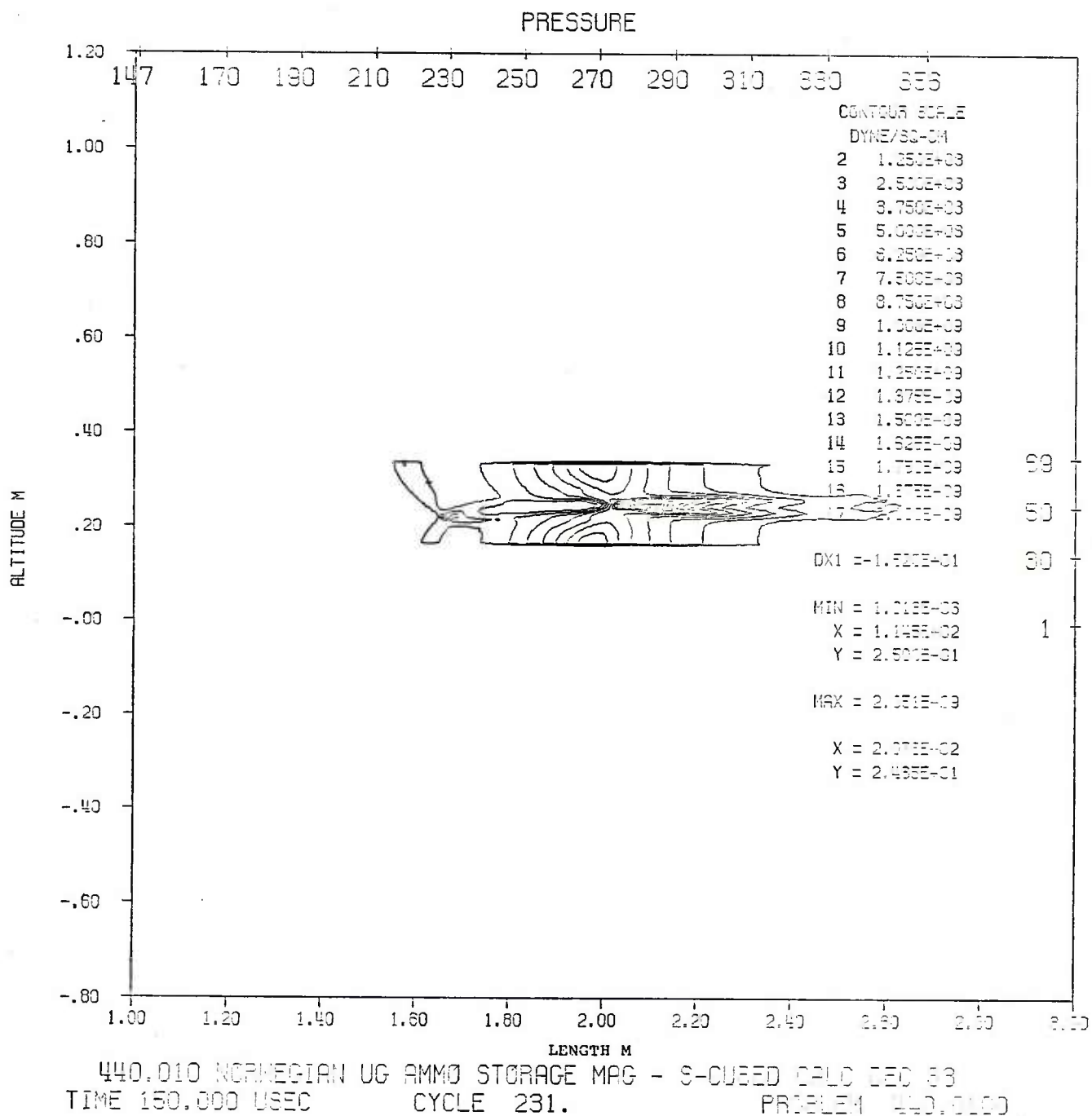


Figure 2. Pressure Contours in Explosive Chamber  
at 150  $\mu$ sec after Detonation

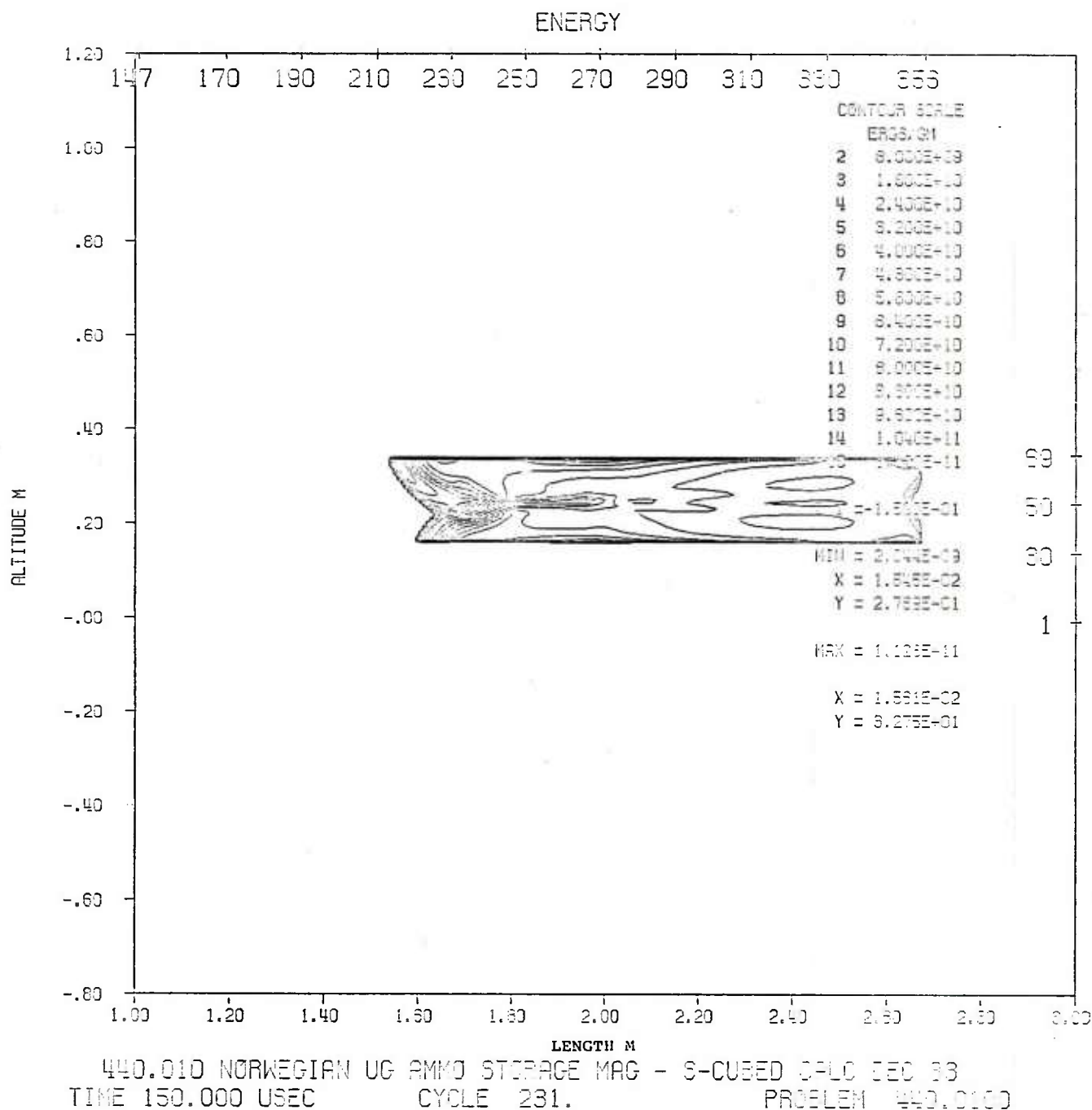
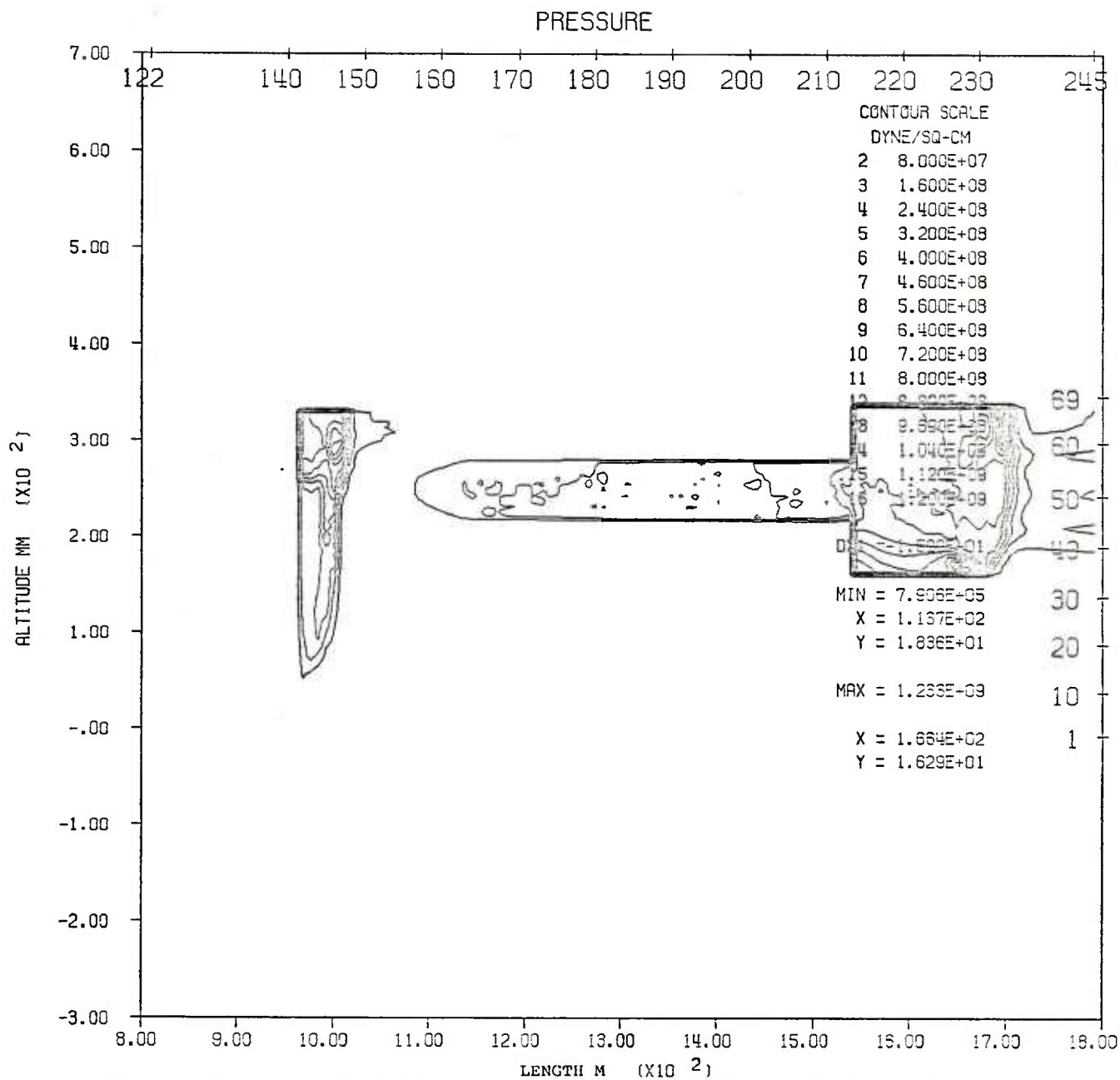


Figure 3. Energy Contours in Explosive Chamber at 150  $\mu$ sec after Detonation



440.010 NORWEGIAN UG AMMO STORAGE MAG - S-CUBED CALC DEC 83  
TIME 339.423 USEC CYCLE 518. PROBLEM 440.0100

Figure 4. Pressure Contours in Vertical Chamber and Passageway at 340  $\mu$ sec after Detonation

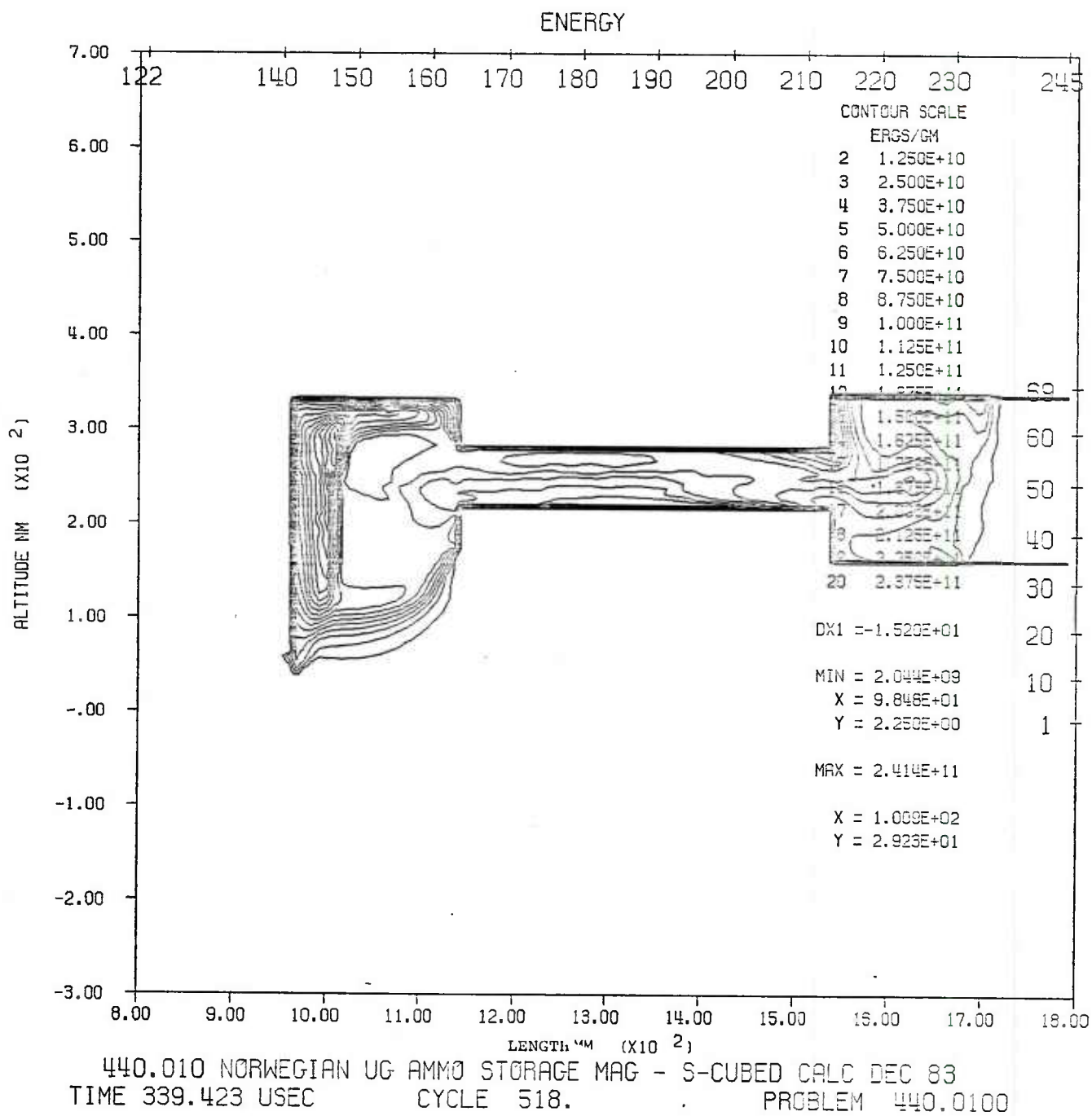
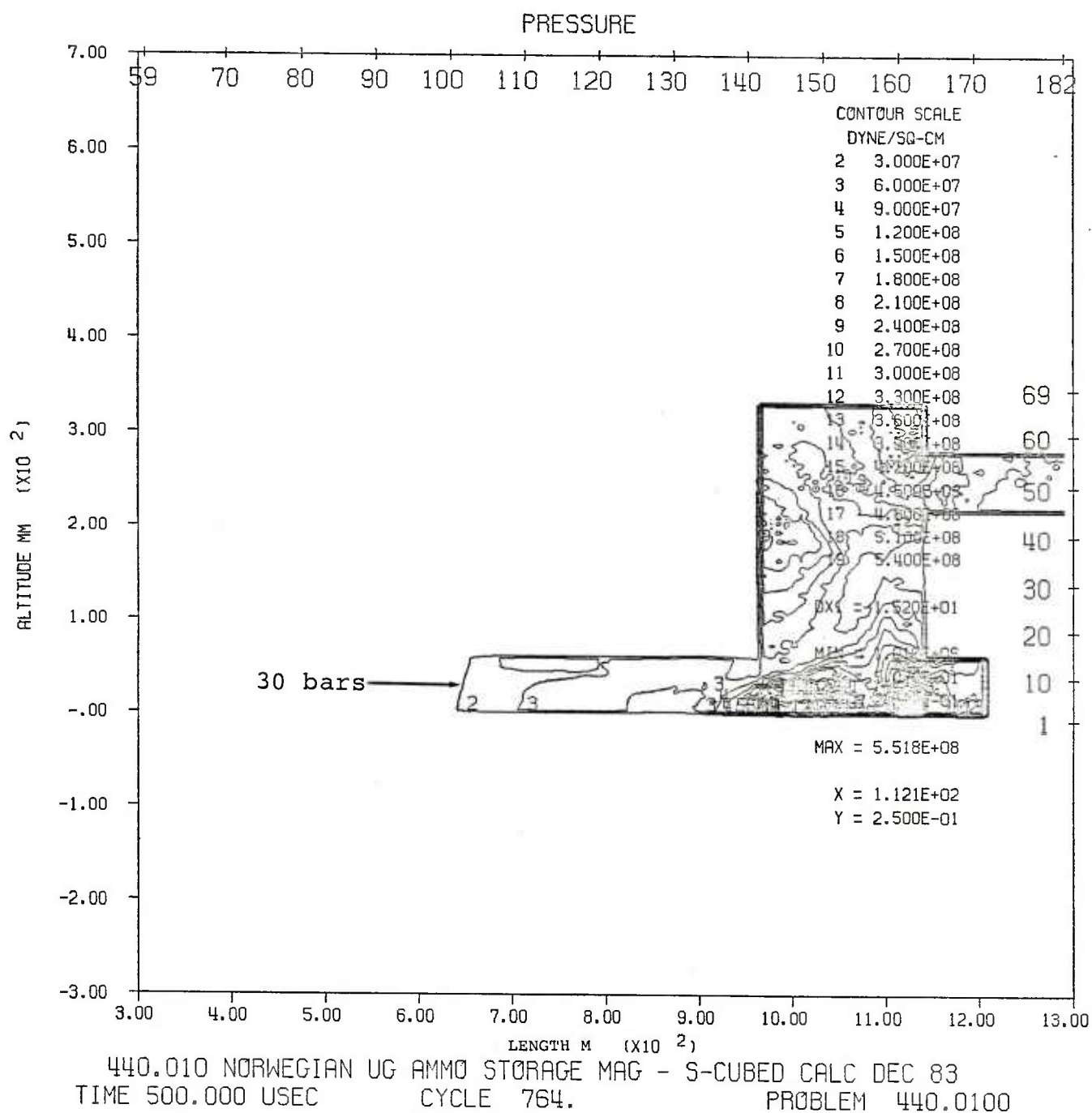
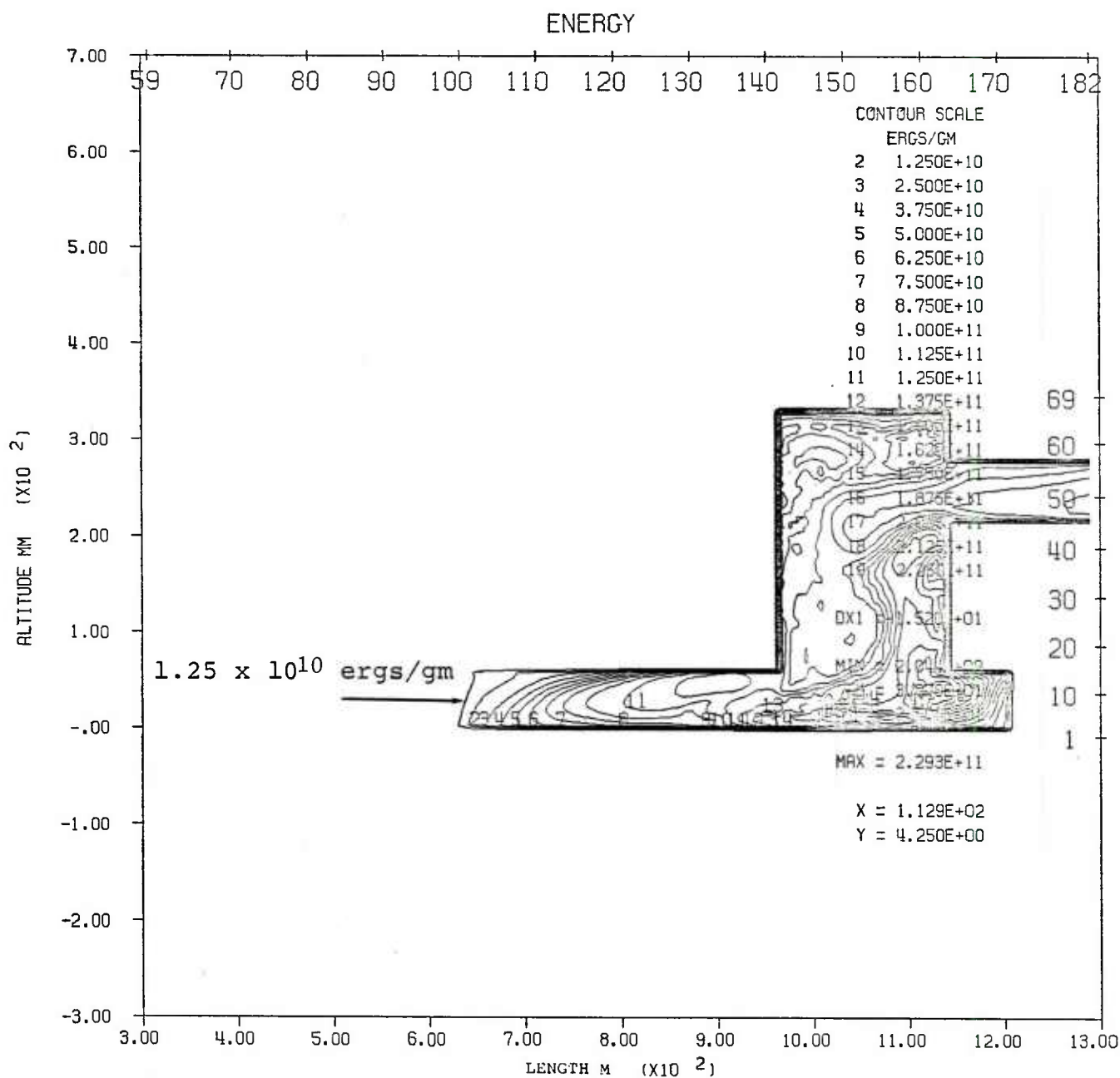


Figure 5. Energy Contours in Vertical Chamber and Passageway at 340  $\mu$ sec after Detonation









440.010 NORWEGIAN UG AMMO STORAGE MAG - S-CUBED CALC DEC 83  
TIME 500.000 USEC CYCLE 764. PROBLEM 440.0100

Figure 7. Energy Contours in Vertical Chamber and Entrance Tunnel at 500 μsec after Detonation

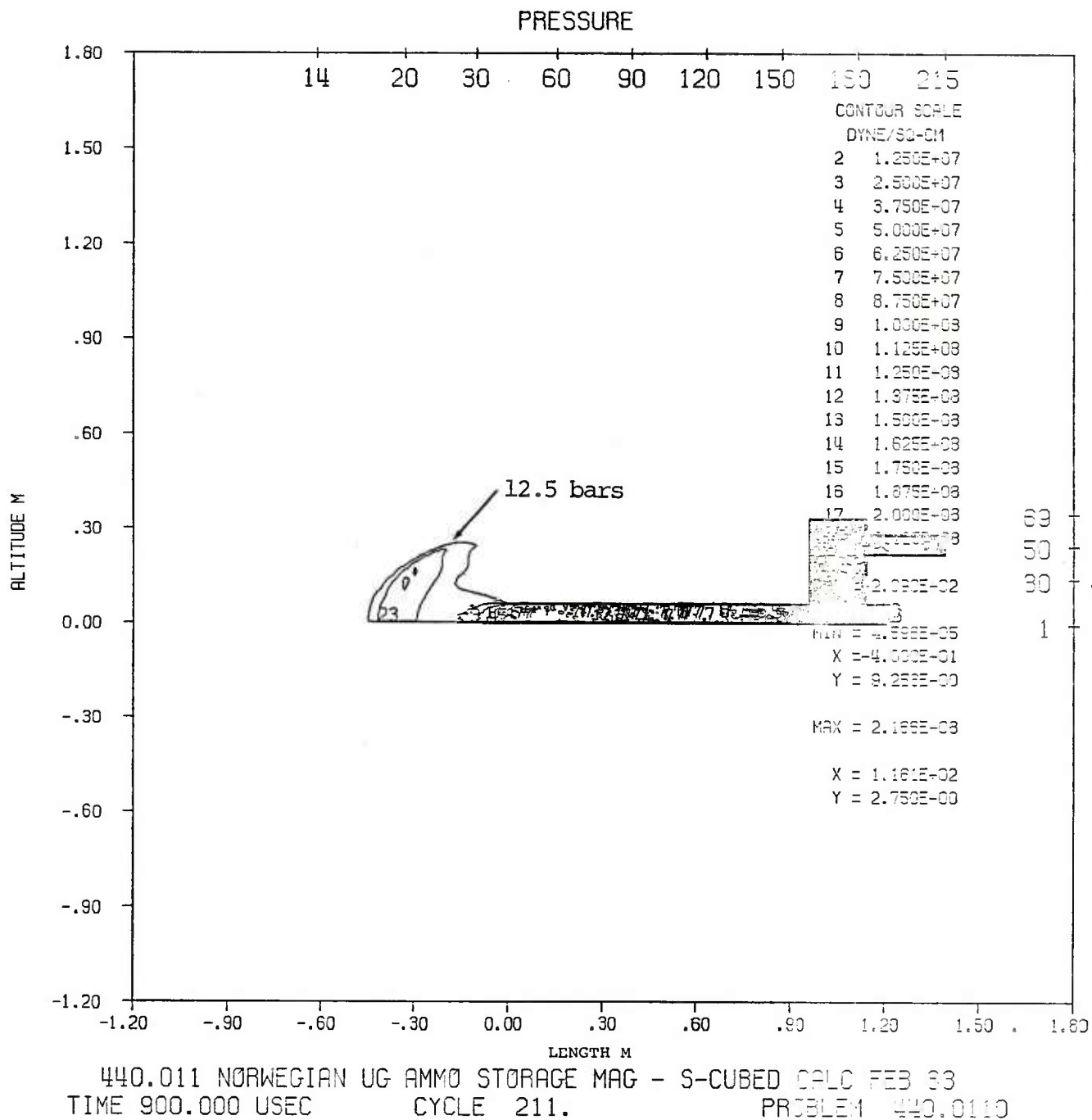


Figure 8. Pressure Contours in Tunnel Entrance Region  
 at 900  $\mu$ sec after Detonation

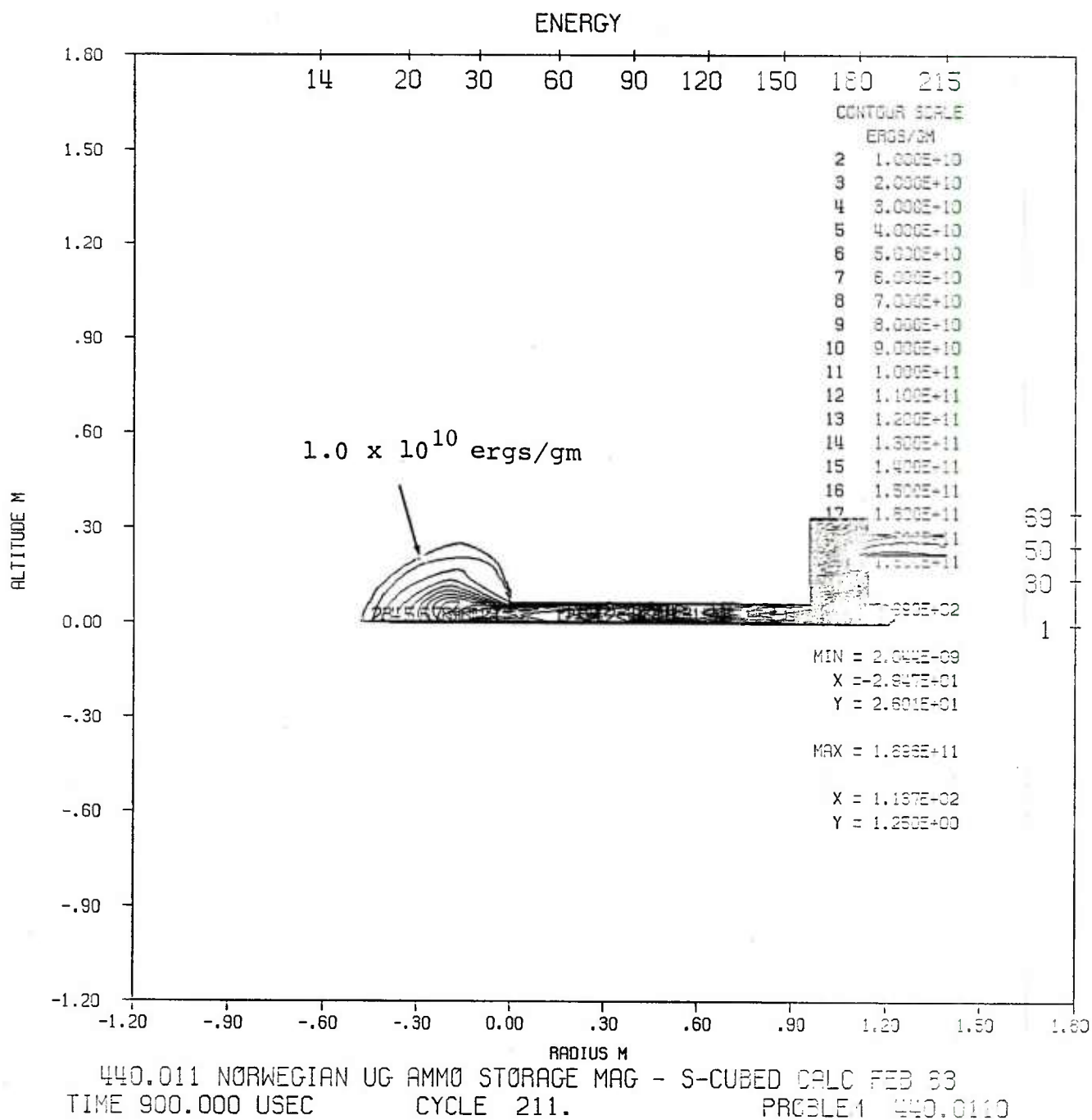
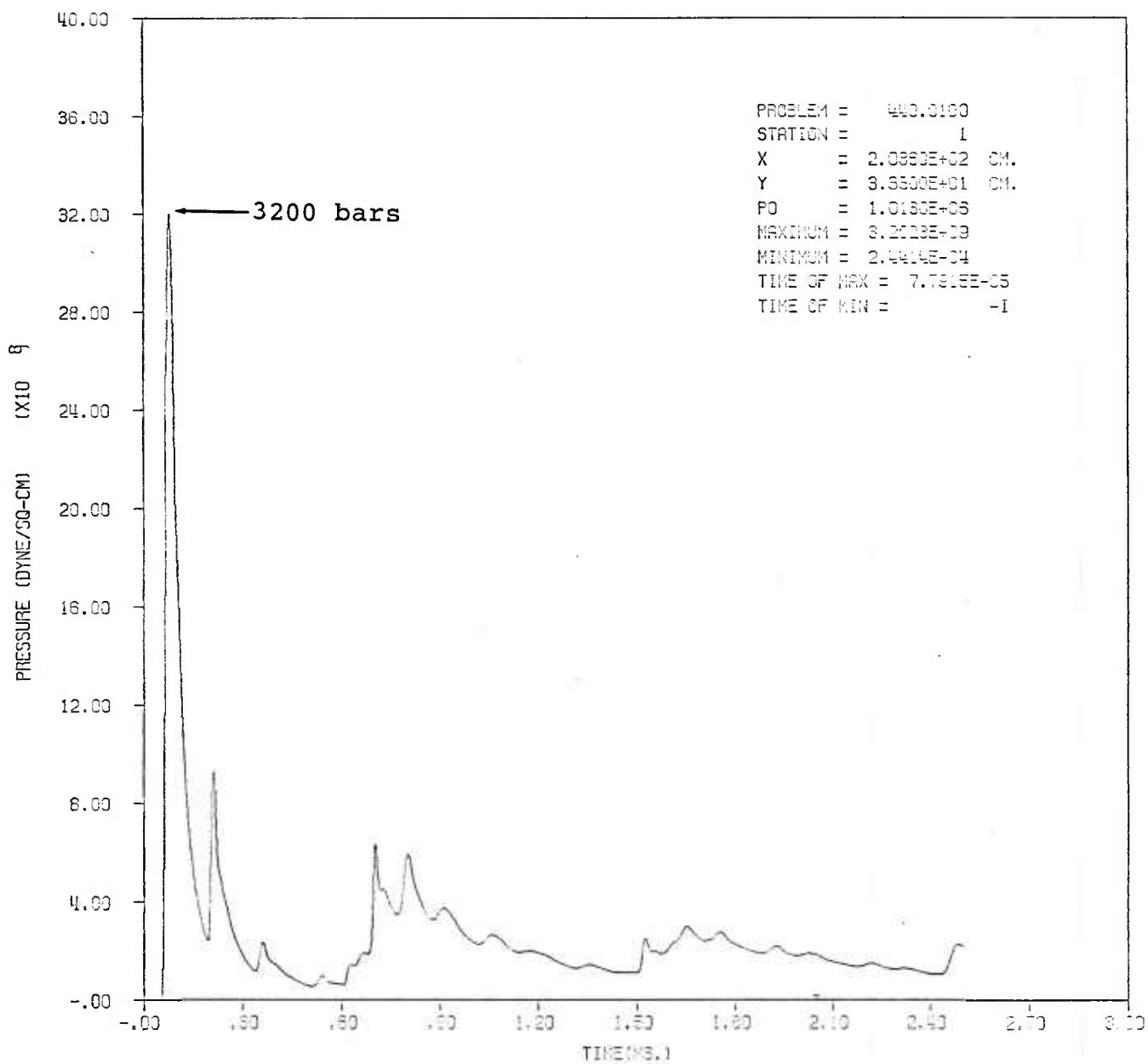


Figure 9. Energy Contours in Tunnel Entrance Region at 900  $\mu$ sec after Detonation

The second type of output is probably of more immediate interest in this application because it is directly comparable to experimental results. "Stations" are predetermined locations in the calculational grid at which hydrodynamic data are monitored as functions of time. For the interior phase calculation, stations were placed at measuring points corresponding to those in the NDCS test. These are the points labeled 1 through 5 in Figure 1. Additional stations were positioned at the tunnel entrance and at other points throughout the calculational grid. Stations 28, 29 and 30 are of particular interest because they are the ones used to drive the second phase of the calculation. Their locations are also shown in Figure 1.

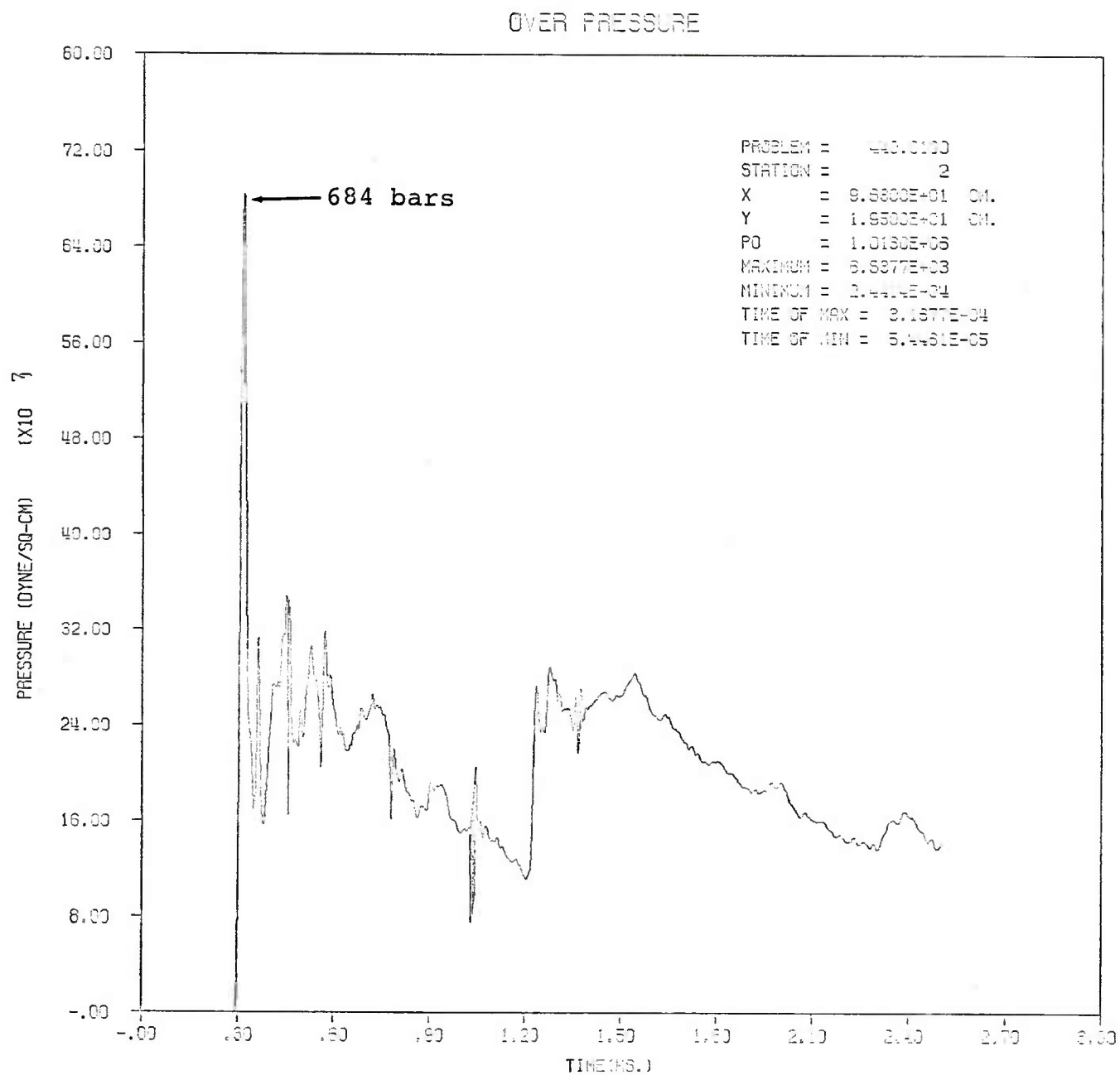
Figures 10 through 14 are overpressure versus time records at Stations 1 through 5. The first three, which are in the explosive and vertical chambers and the connecting tunnel between them, show a large initial spike followed by many smaller peaks. The latter are due to reflections from the chamber walls. Stations 4 and 5, for which the overpressure records are shown in Figures 13 and 14, are located in the entrance tunnel. The records show many sharp spikes, which are a result of the mixture of air and detonation products flowing in this region. The maximum overpressure in the entrance tunnel is about 80 bars. At Measuring Point 5, the density versus time record is given in Figure 15.

# OVER PRESSURE



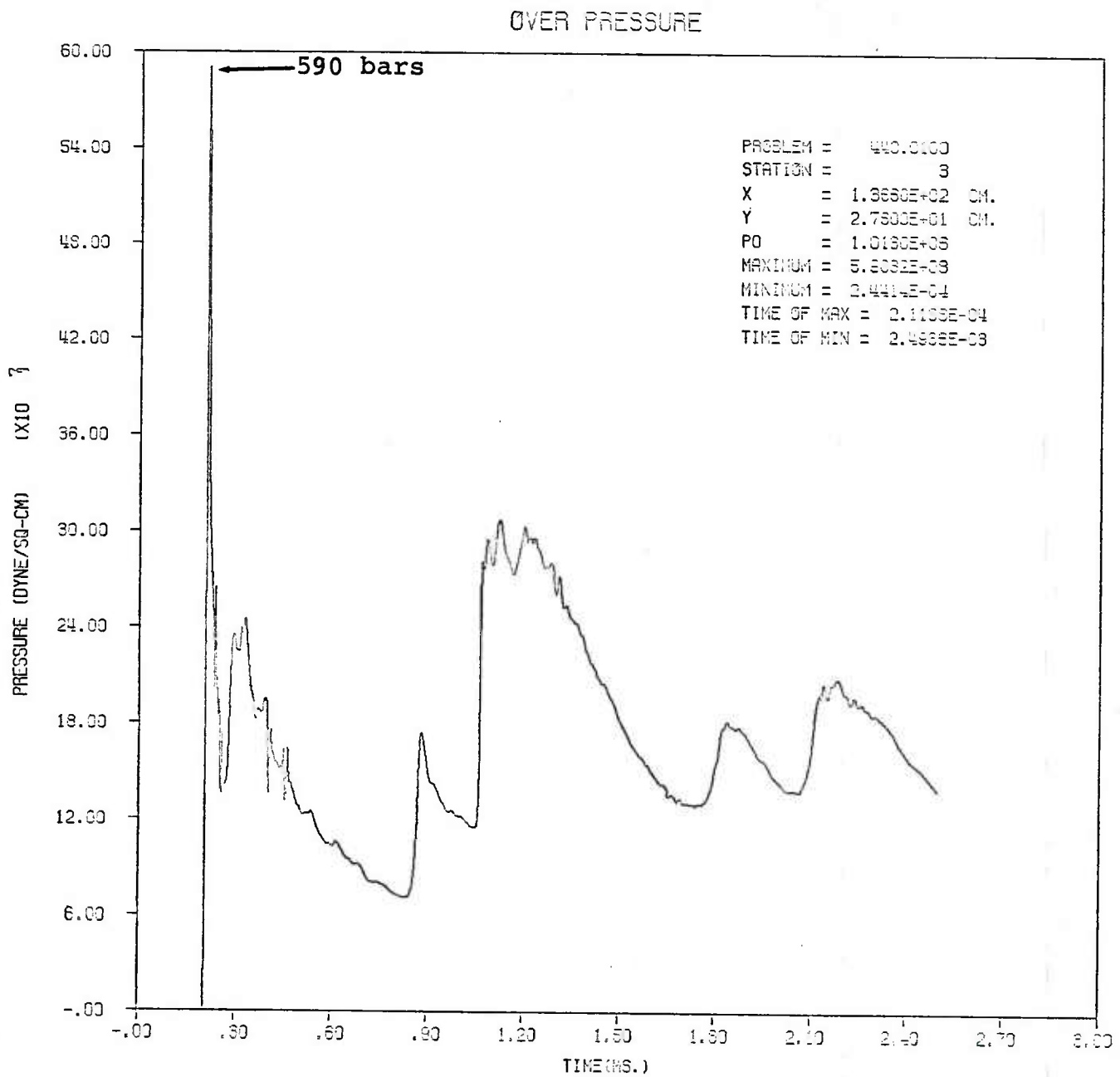
440.010 NORWEGIAN UG RNM43 STORAGE MPG - 3-CUBED CALC DEC 23

Figure 10. Overpressure versus Time Record at Measuring Point 1



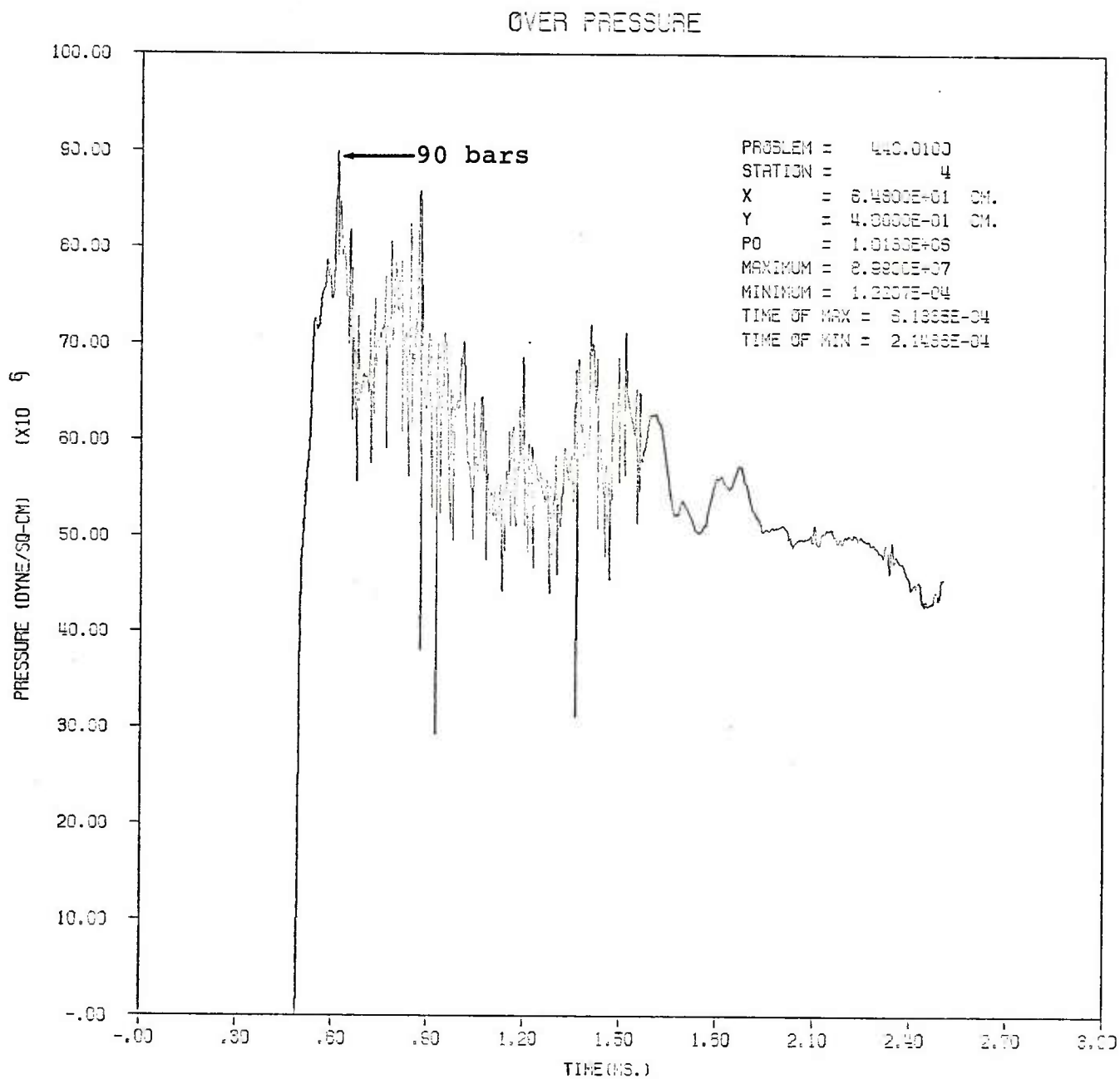
440.010 NORWEGIAN UG R/W STORAGE MAG - S-CUBED CALC DEC 83

Figure 11. Overpressure versus Time Record at Measuring Point 2



440.010 NORWEGIAN UG RIMMO STORAGE MAG - S-CUBED CALD DEC 83

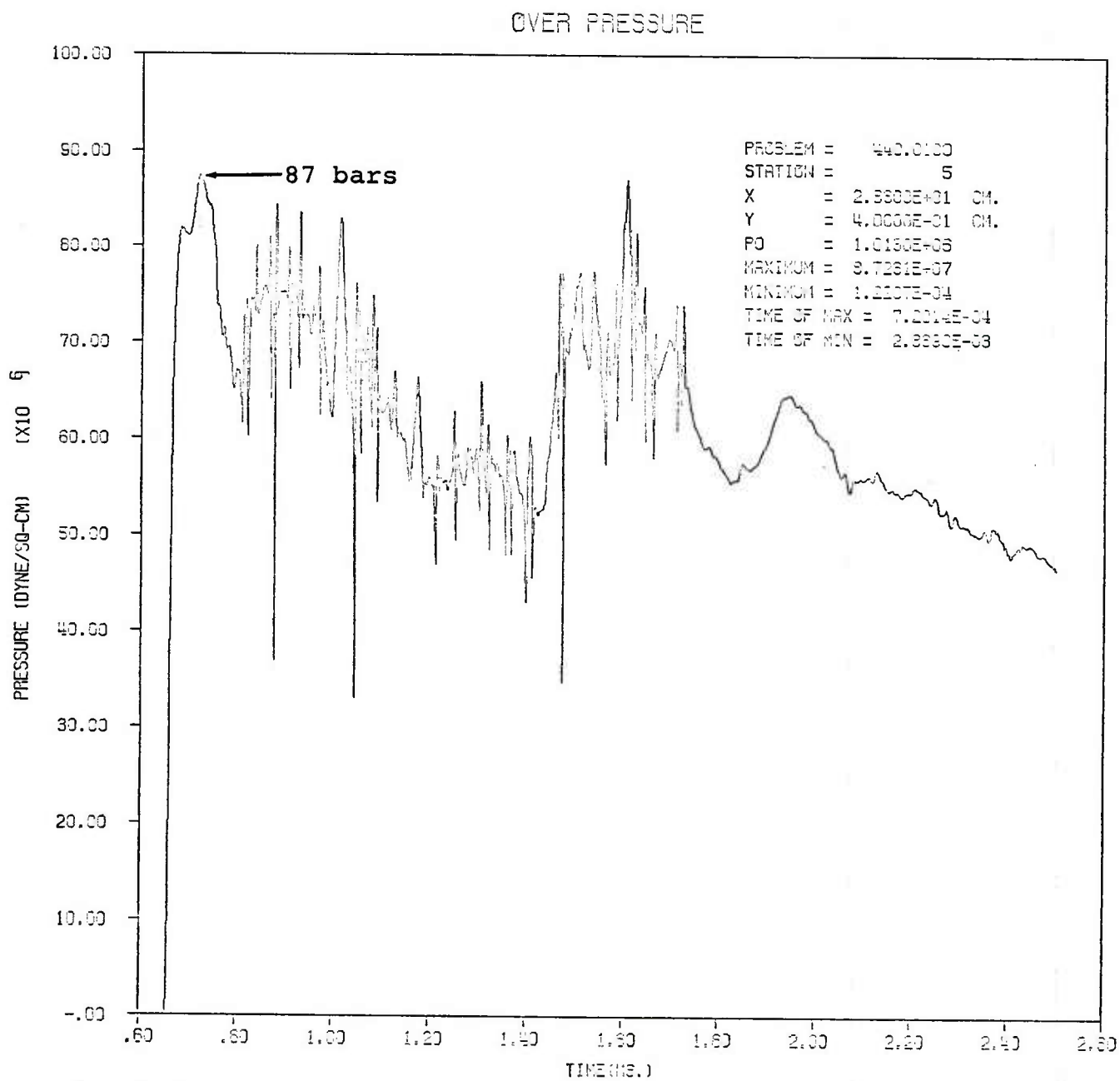
Figure 12. Overpressure versus Time Record at Measuring Point 3



440.010 NORWEGIAN UG AMMO STORAGE MAG - S-CUBED CALC DEC 83

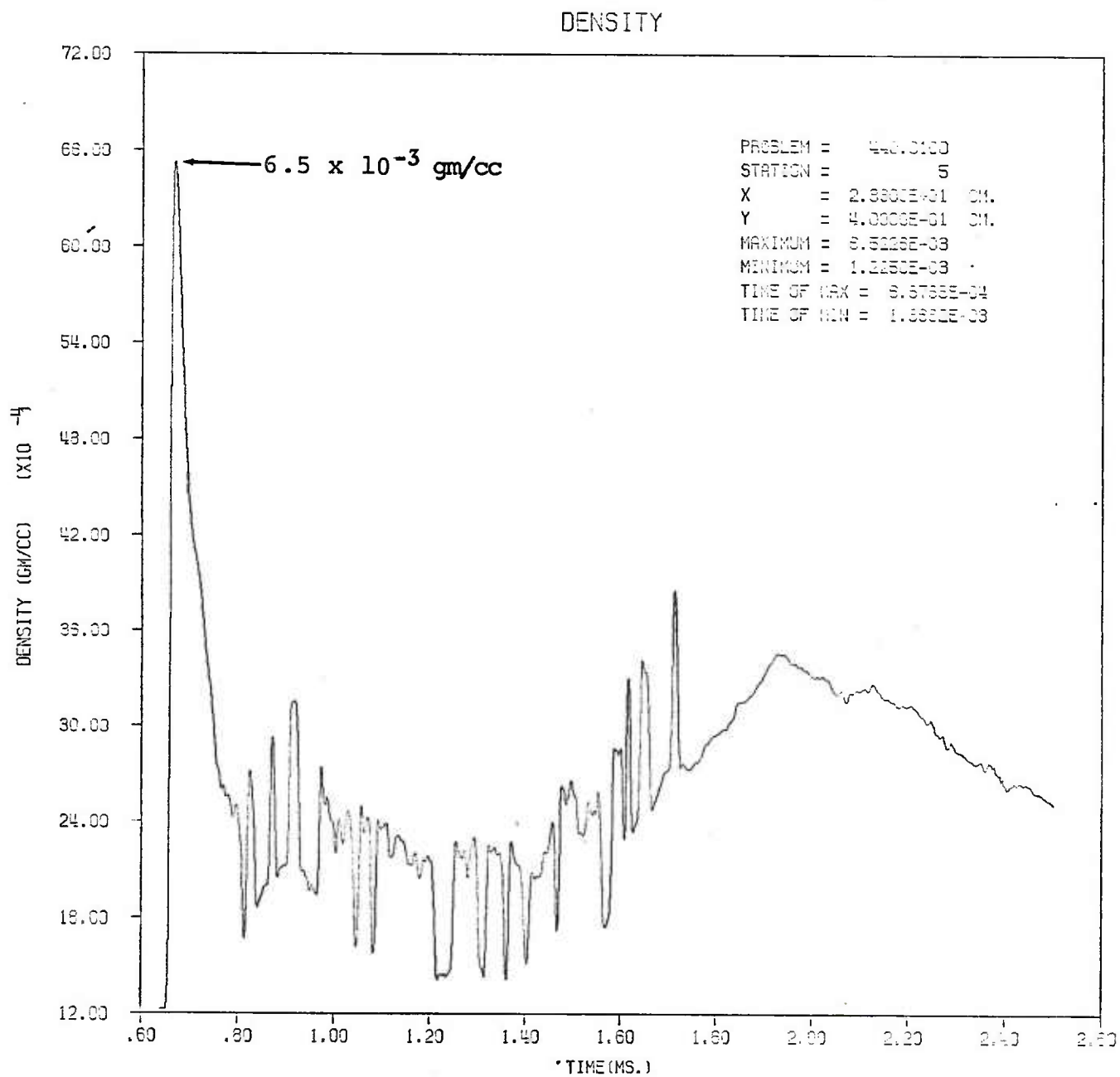
**Figure 13. Overpressure versus Time Record at Measuring Point 4**





440.010 NORWEGIAN UG AMMO STORAGE MAG - S-CUBED OPLC DEC 83

Figure 14. Overpressure versus Time Record at Measuring Point 5

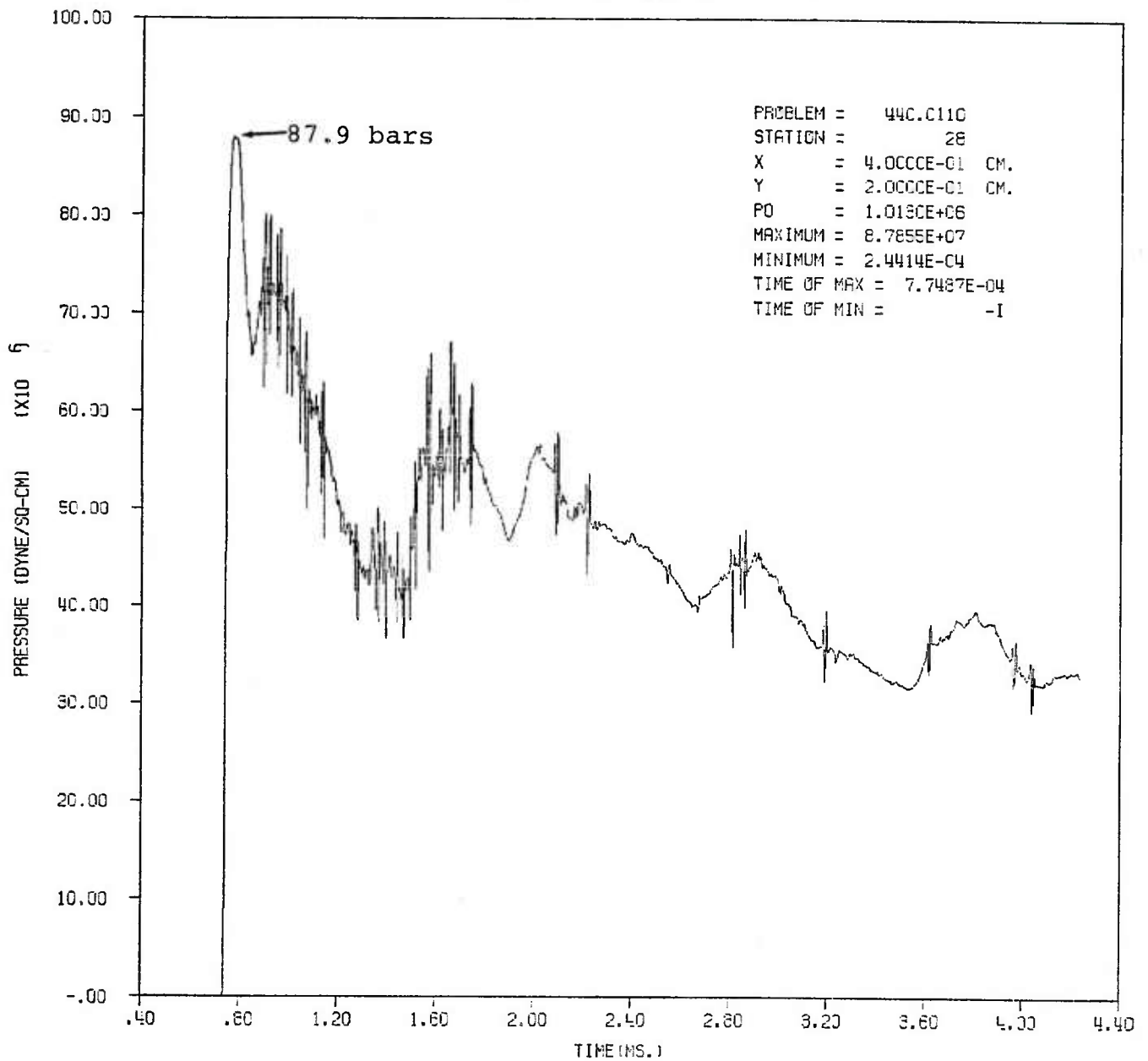


440.010 NORWEGIAN UG AMMO STORAGE MAG - S-CUBED CALC DEC 83

Figure 15. Density vs. Time Record at Measuring Point 5

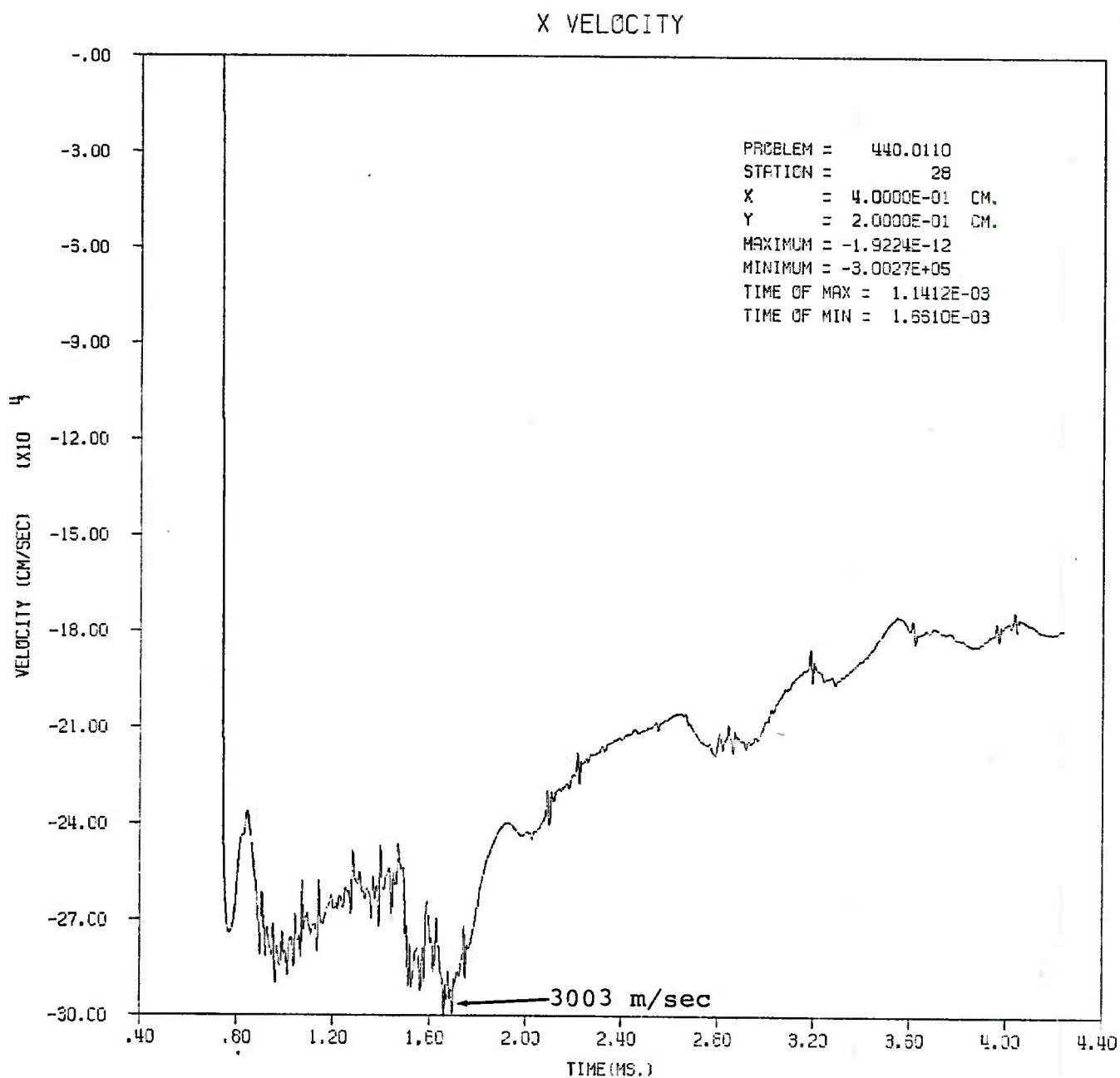
Parameters at the tunnel entrance (Stations 28, 29 and 30) are shown in Figures 16 through 21. For these stations, the horizontal flow velocities versus time are given as well as the overpressures. Note that these velocities are negative because flow through the portal is in the "-x" direction.

# OVER PRESSURE



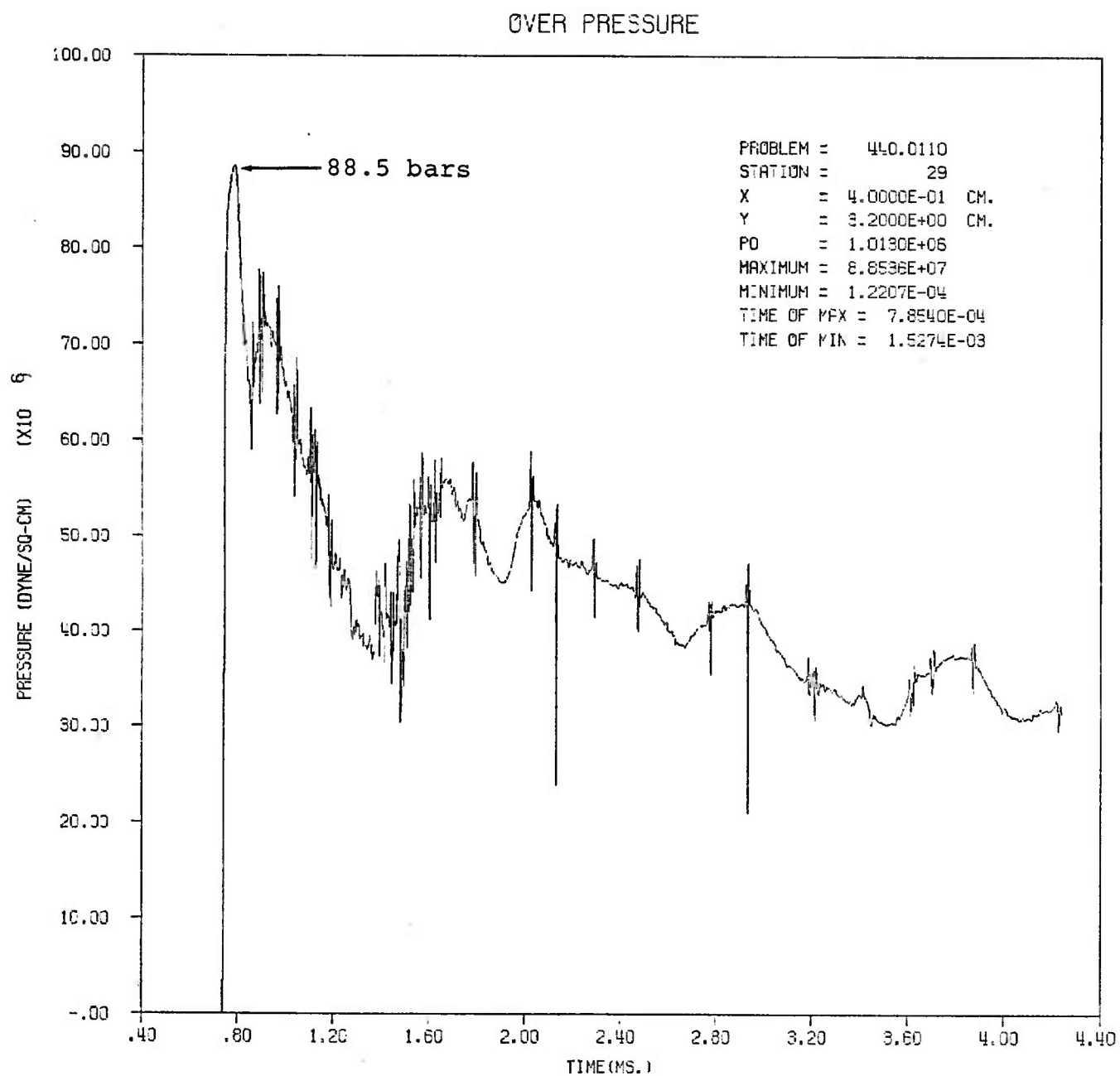
440.011 NORWEGIAN UG AMMO STORAGE MAG - S-CUBED CALC FEB 83

Figure 16. Overpressure versus Time Record at Tunnel Entrance, Near the Floor



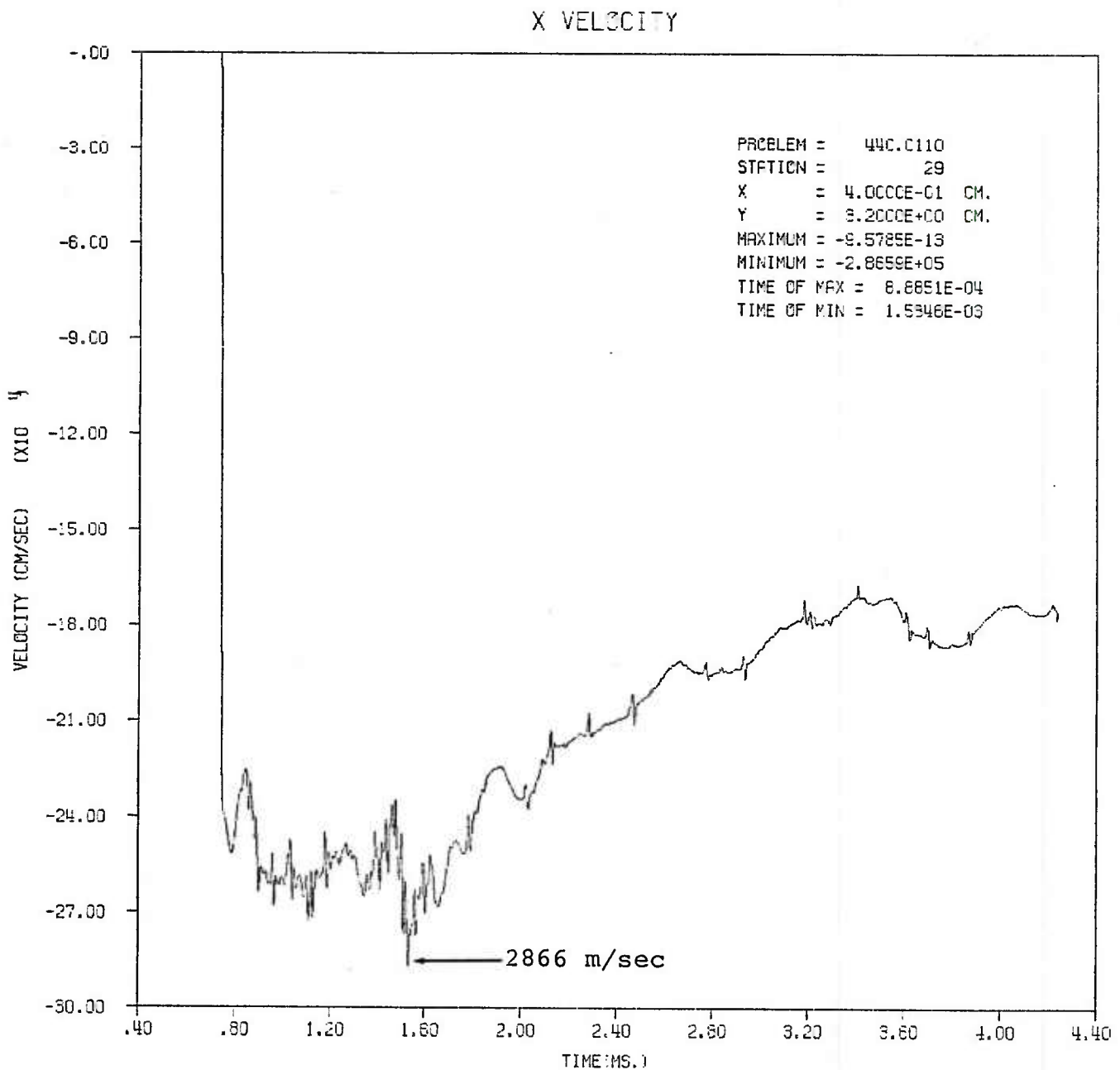
440.011 NORWEGIAN LG AMMO STORAGE MPG - S-CUBED CALC FEB 83

Figure 17. Horizontal Velocity versus Time Record at Tunnel Entrance, Near the Floor



440.011 NORWEGIAN UG AMMO STORAGE MAG - S-CUBED CALC FEB 83

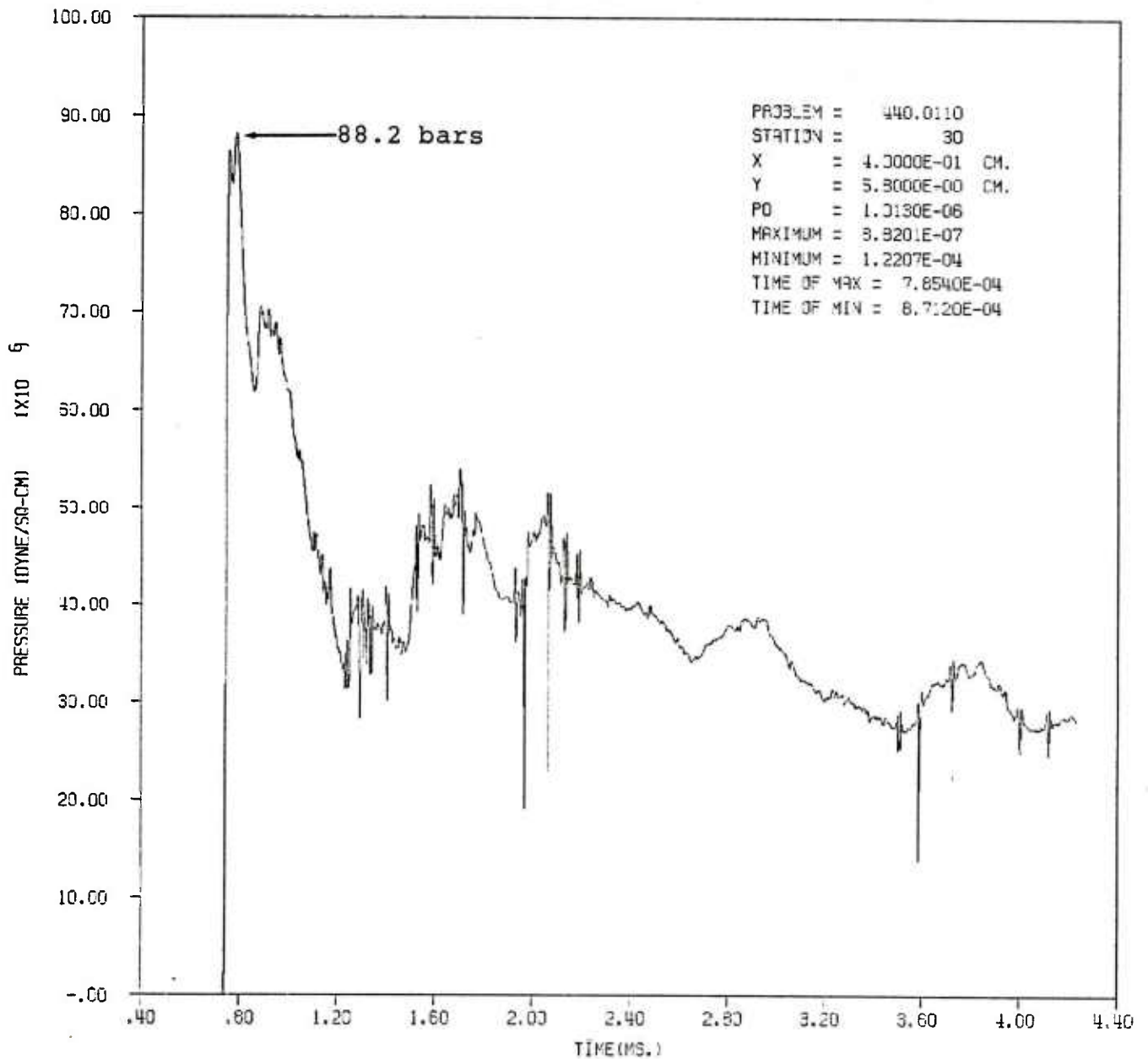
Figure 18. Overpressure versus Time Record at Tunnel Entrance, Near the Center



440.011 NORWEGIAN UG AMMO STORAGE MAG - S-CUBED CALC FEB 83

Figure 19. Horizontal Velocity versus Time Record at Tunnel Entrance, Near the Center

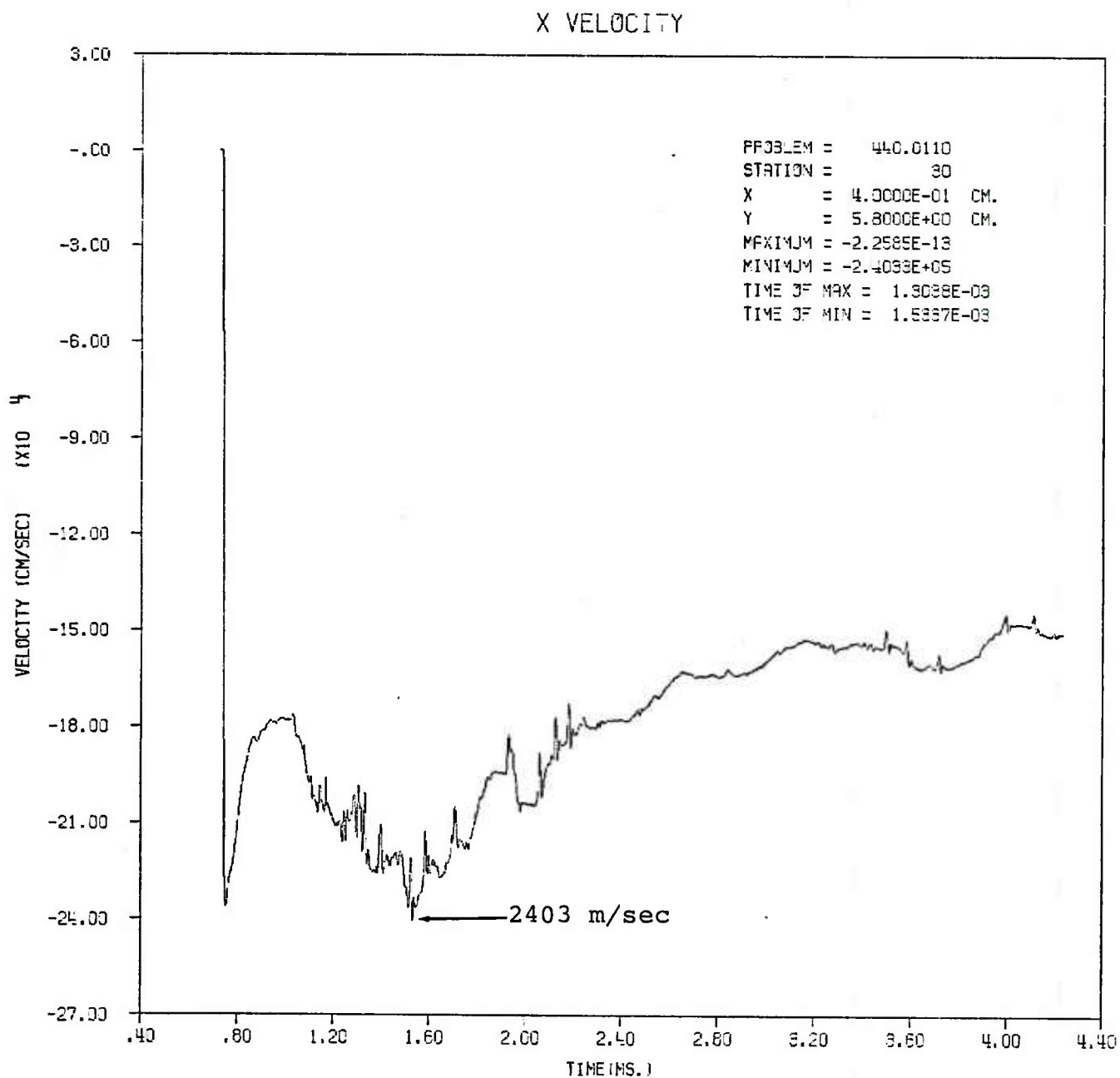
# OVER PRESSURE



440.011 NORWEGIAN UG AMMO STORAGE MAG - S-CUBED CALC FEB 83

Figure 20. Overpressure versus Time Record at Tunnel Entrance, Near the Roof





440.011 NORWEGIAN UG AMMO STORAGE MAG - S-CUBED CALC FEB 83

Figure 21. Horizontal Velocity versus Time Record at Tunnel Entrance, Near the Roof

### III. PHASE 2: EXPANSION INTO EXTERIOR REGION

In order to model the exterior region, a computational mesh was set up using cylindrical coordinates. The mesh consists of 182x176 zones, for a total of 31,304. The overall grid dimensions are 5.96 m by 5.99 m. A 100x100 cell subgrid, in which the size of each cell is approximately 0.49x0.8 cm, was defined on the cylindrical axis at the tunnel opening. Beyond the subgrid, cell size is expanded by about 5 percent per cell in each direction. Stations were located at intervals along radial lines from the tunnel exit.

The configuration is illustrated in Figure 22. For this phase, a plane through the axis of symmetry, which can be thought of as a flat, perfectly reflecting surface, becomes the ground plane. The tunnel opening and cliff face become cylindrical sections when converted from Cartesian to cylindrical coordinates. The radius of the opening was adjusted so that the cross-sectional area of the half-disk opening in cylindrical coordinates is equal to the rectangular 5x6 cm tunnel opening of Phase 1.

The cliff face was modeled by placing a row of "island" cells along the bottom of the mesh. An island is a non-compressible, reflective cell of the same type as were used in Phase 1 for the tunnel walls. The configuration, it should be noted, is rotated by 90 degrees from that of Phase 1, so that direction of flow is upward in Figure 22.

The calculation was initiated at 0.7 msec by setting the hydrodynamic parameters in the cells at the tunnel opening to those read from the station records of Phase 1. To perform the transformation, the "-x" velocities of the Phase 1 station records became the "+y" velocities of the Phase 2 driver cells,

and +y's became +x's. Interpolation was performed to drive the cells at locations between stations at appropriate values.

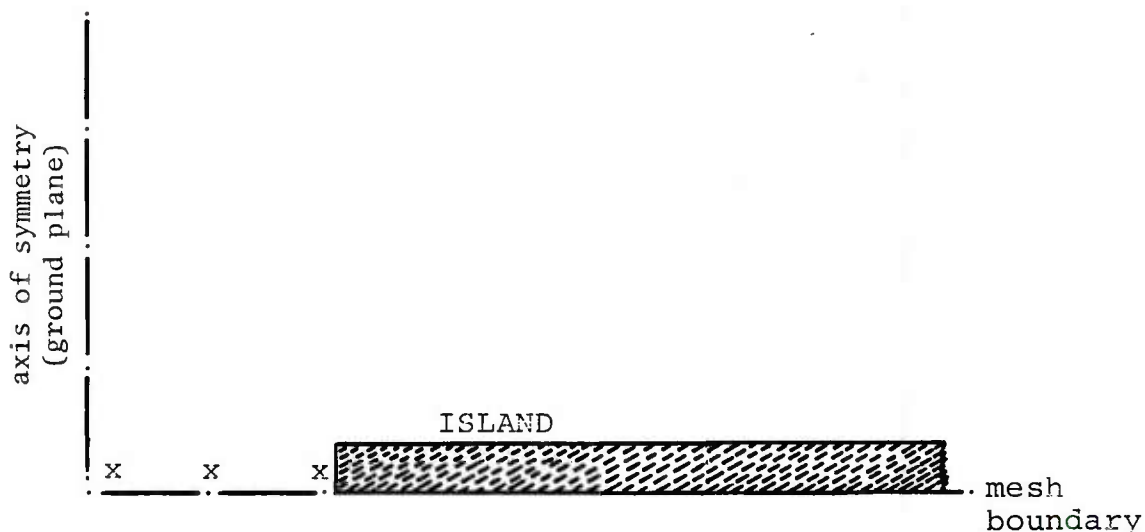


Figure 22. Calculational Configuration for Phase 2

The second phase calculation was run to 3.1 msec after detonation of the explosive. By this time, the shock wave emerging from the tunnel opening had traveled a distance of 1.75 m (5.74 ft) along the axis and had decayed to an over-pressure of approximately 1.0 bar (14.5 psi). Figures 23 through 28 illustrate the pressure, density, and energy at two different times (1.5 and 2.3 msec) during the calculation. An interesting feature shown by the pressure and density plots is the development of a Mach-stem-like structure at the interaction with the cliff face. The structure, usually observed only with height-of-burst detonations, is an indication of flow toward the surface (downward in the picture) as well as parallel to the surface.

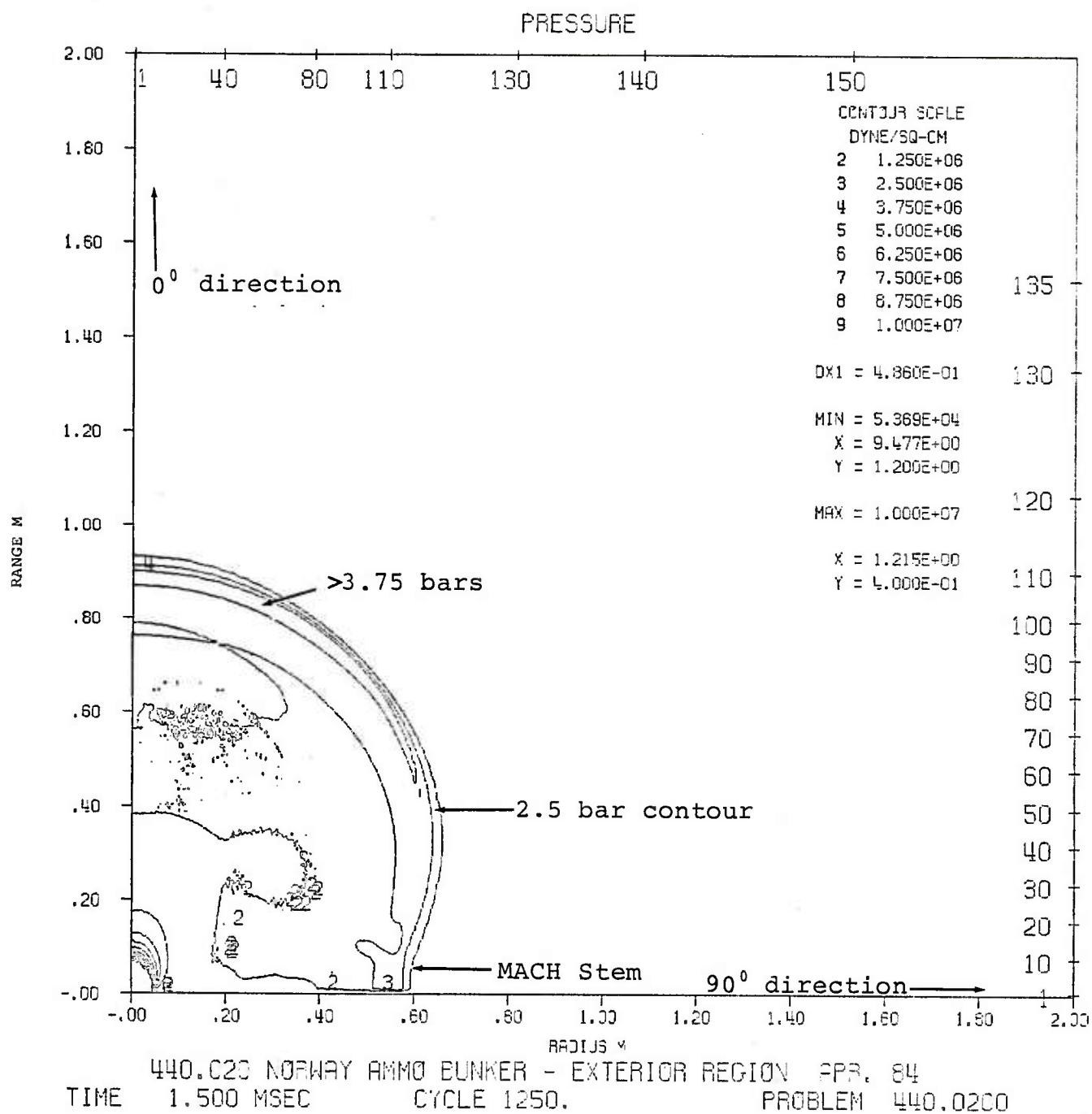


Figure 23. Pressure Contours in Exterior Region at 1.5 msec after Detonation

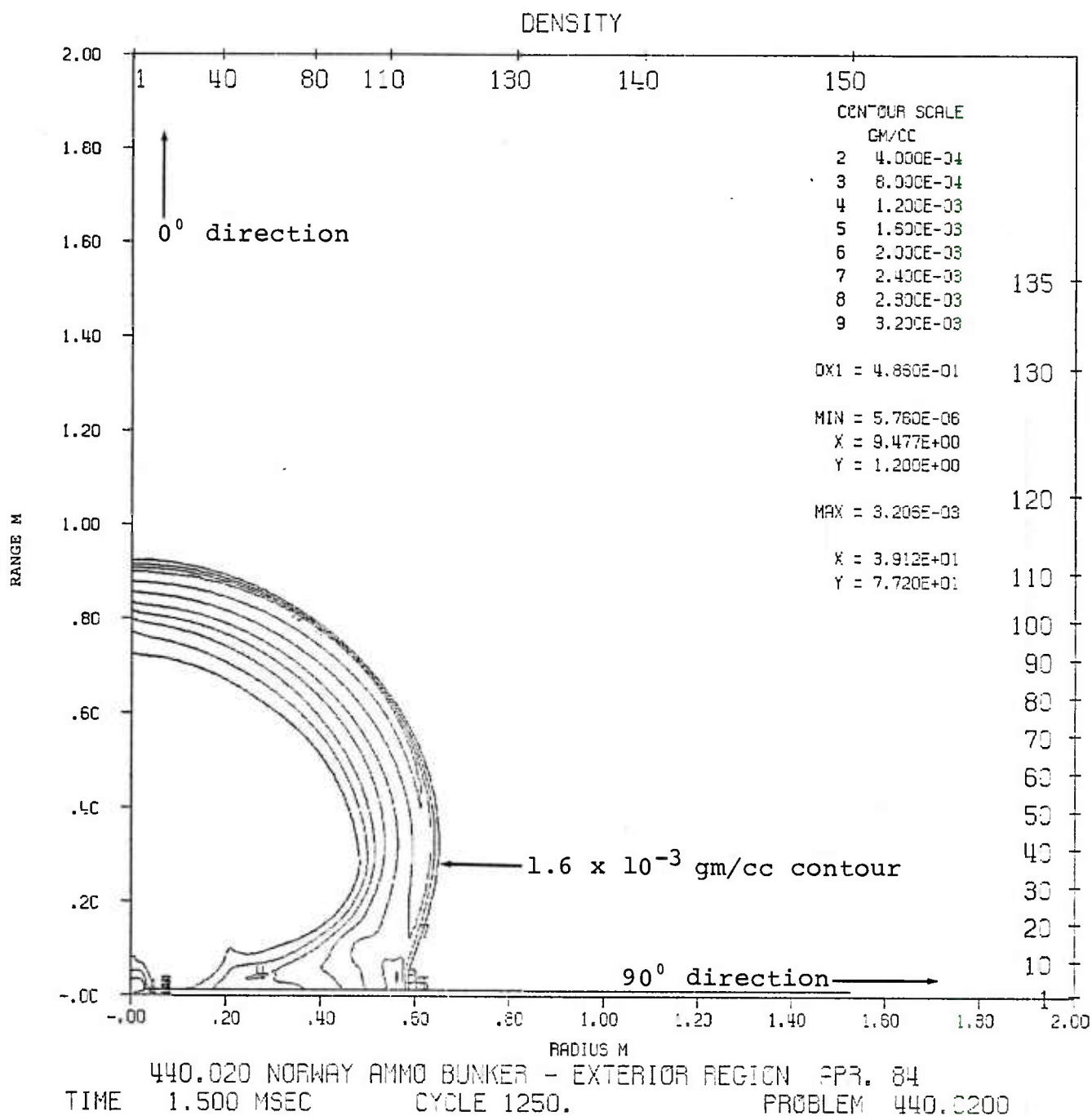


Figure 24. Density Contours in Exterior Region at 1.5 msec after Detonation

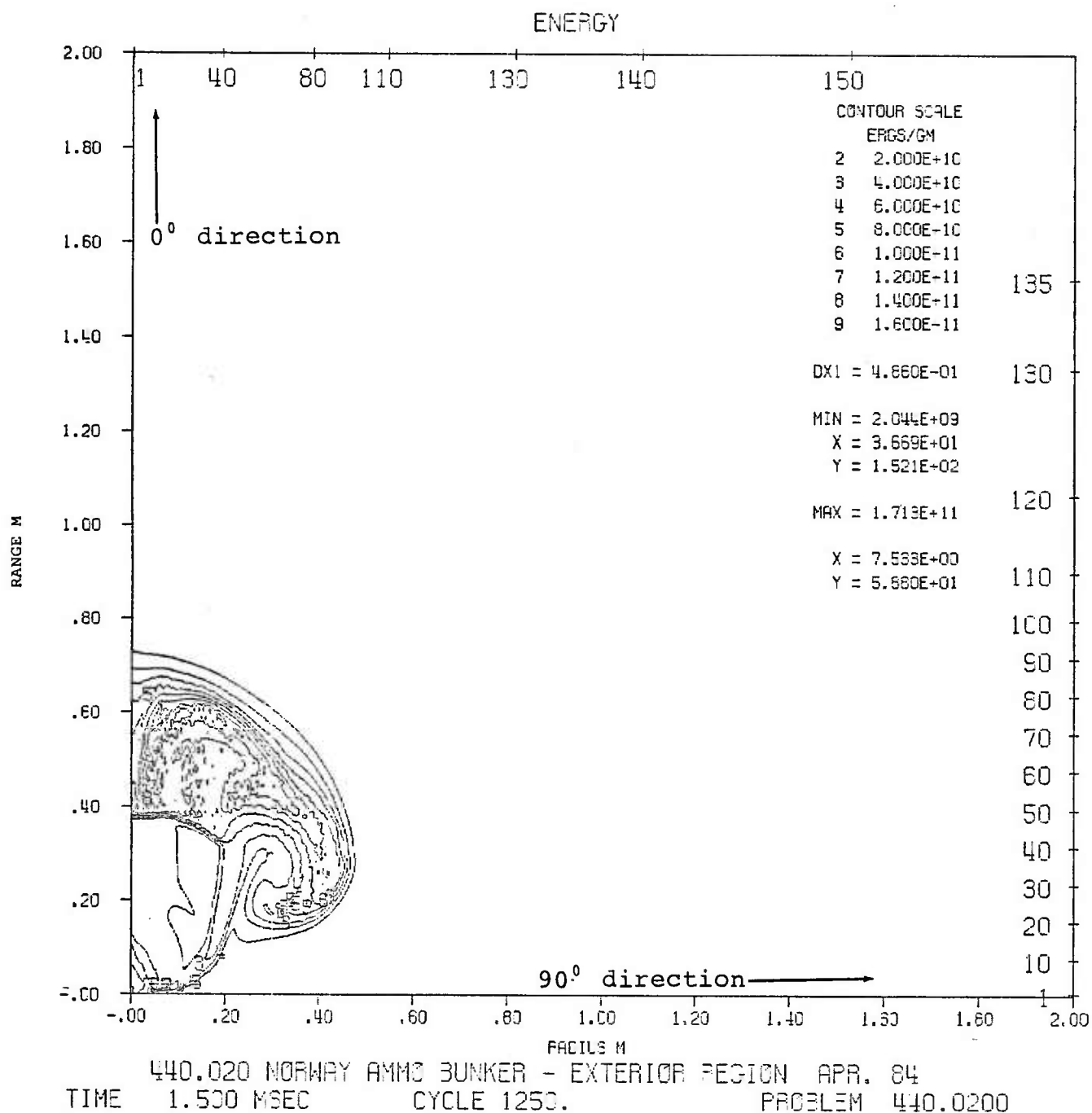


Figure 25. Energy Contours in Exterior Region at 1.5 msec after Detonation

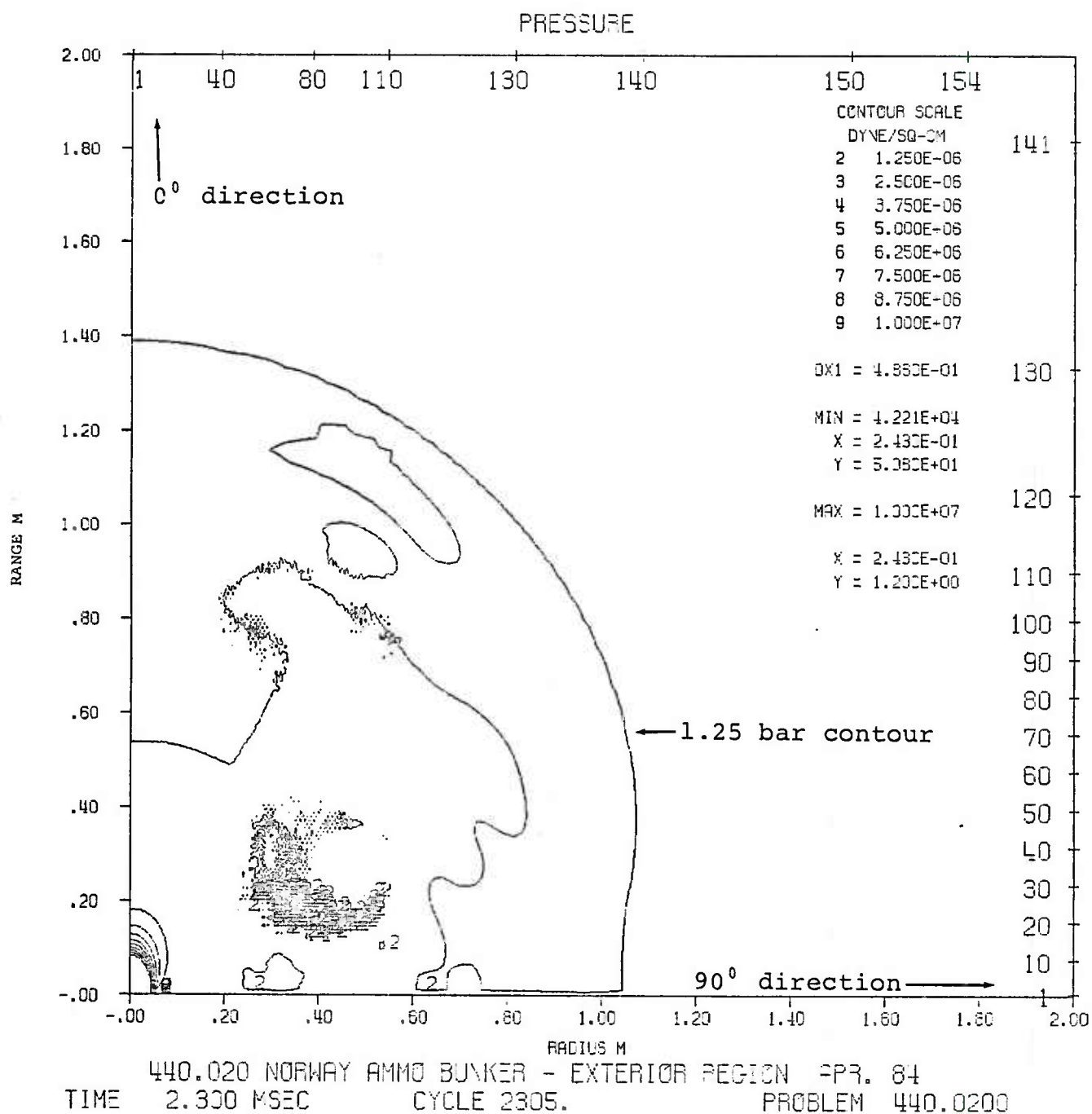


Figure 26. Pressure Contours in Exterior Region at 2.3 msec after Detonation

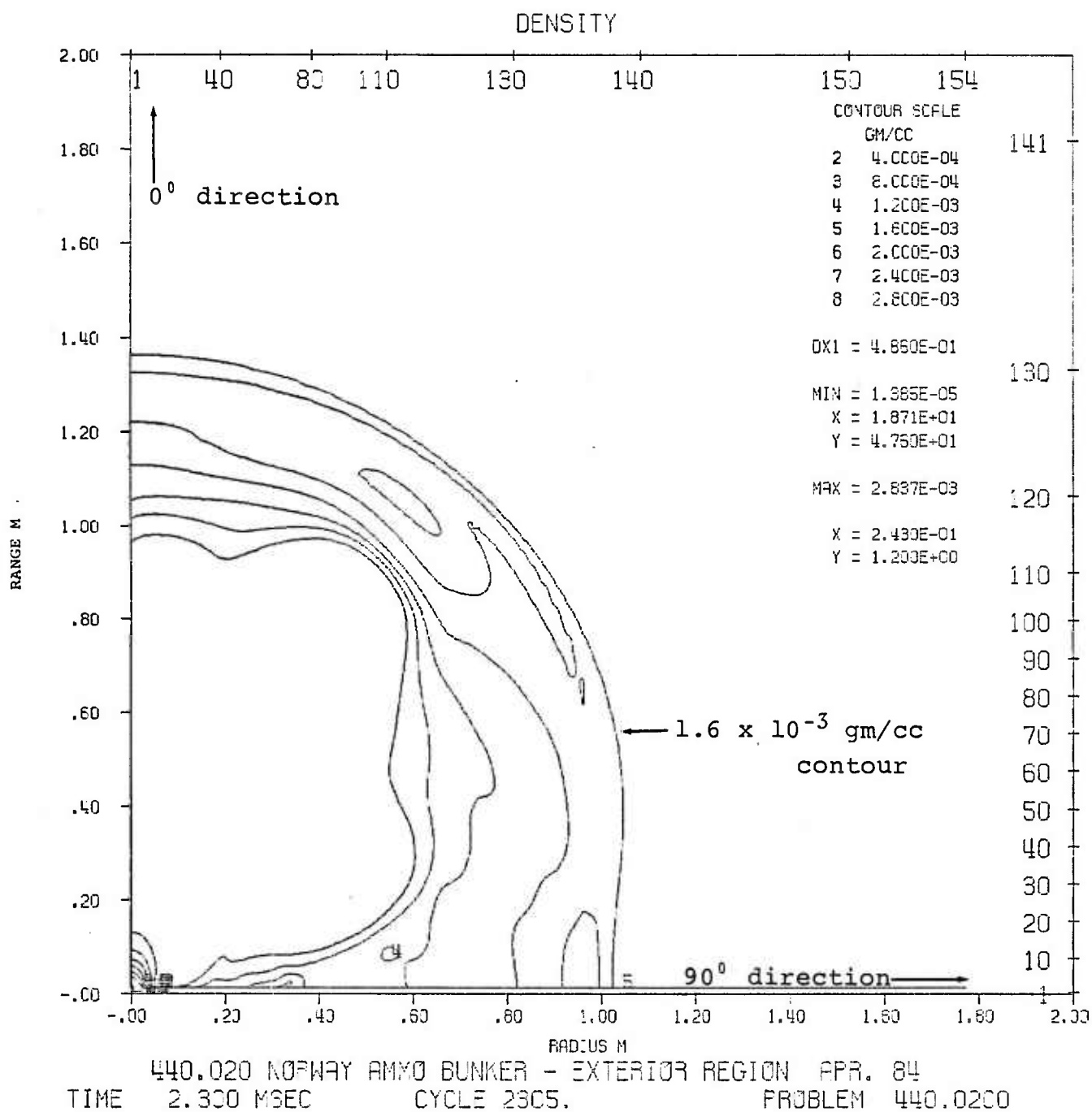


Figure 27. Density Contours in Exterior Region at 2.3 msec after Detonation



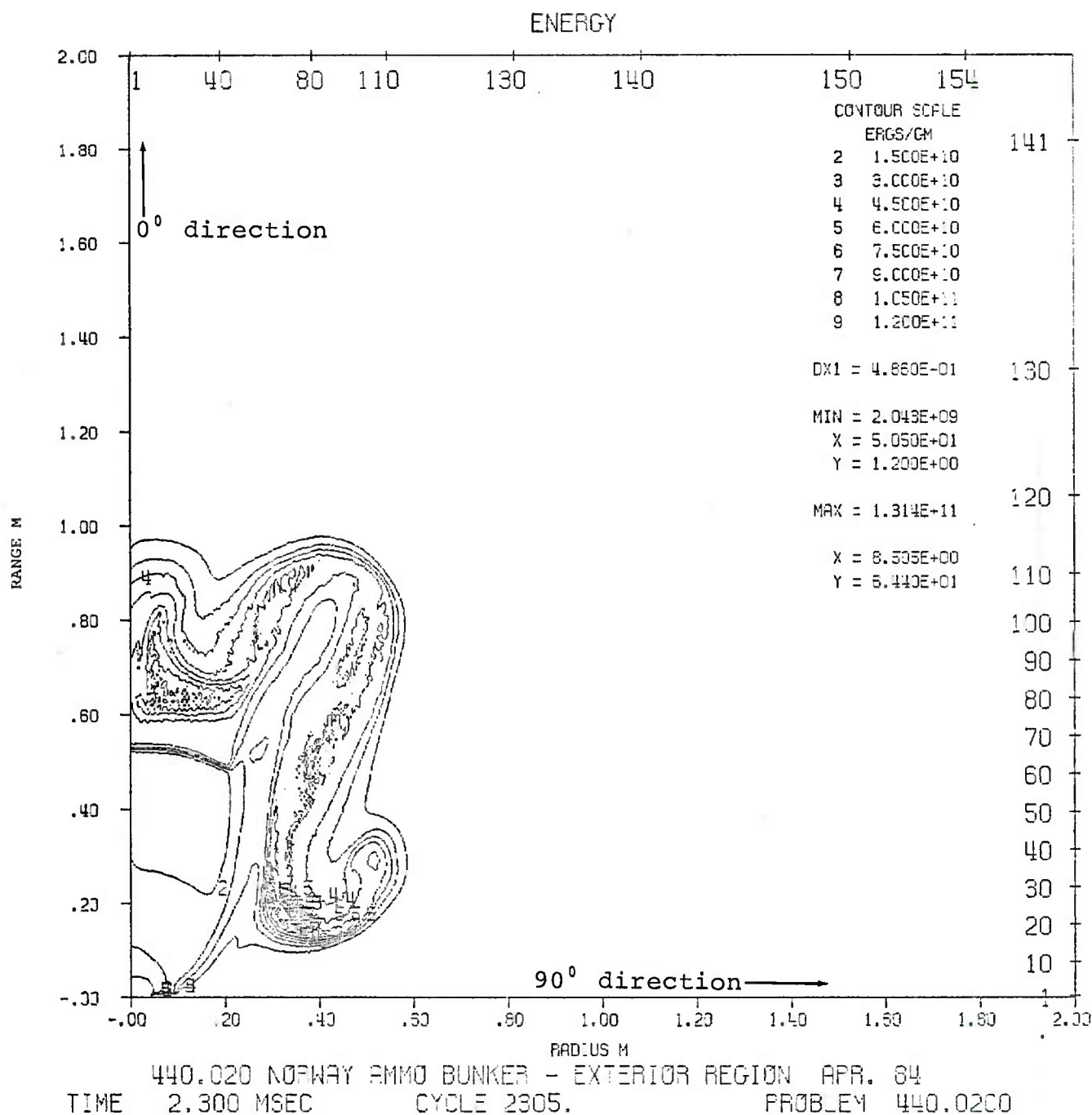


Figure 28. Energy Contours in Exterior Region at 2.3 msec after Detonation

#### IV. PHASE 3: ONE-DIMENSIONAL CALCULATIONS

Phase 3 consists of a series of one-dimensional calculations along lines radiating from the tunnel entrance. The Phase 3 calculations were done using SAP (Spherical Air Puff), S-CUBED's version of the one-dimensional Eulerian, spherical-symmetry hydrocode originally developed at the Air Force Weapons Laboratory (AFWL).

At 3.1 msec, as previously mentioned, the Phase 2 two-dimensional calculation was terminated. It was replaced by a series of one-dimensional calculations along the lines A through G shown in Figure 29. The initial conditions for each Phase 3 calculation were obtained by "cutting" through the Phase 2 calculational mesh at 3.1 msec. Energy, density and velocity values were read from zones through which the lines passed. Interpolation across four adjacent zones was performed in order to obtain values along the lines. Also, the component x and y velocities were combined to determine the appropriate velocity in the direction of the line cut. Phase 2 contour plots at 3.1 msec, which were used to provide the initial conditions, are given in Figures 30 through 33. The lines along which the cuts were taken (approximately every 15 deg) are shown in Figure 30.

As each of the SAP calculations proceeded in time, the waveform defined by the cut was allowed to propagate outward. The innermost cell was continually reset to conditions from the late-time record for Station 29 (Phase 1). The one-dimensional calculations were continued until a shock front peak over-pressure of less than 250 mbar, or 3.62 psi, was reached. This occurred at times between 12.0 and 12.5 msec. After 4.2 msec, when the Station 29 record ended, constant values of the

parameters equal to those at the last time for Station 29 (4.2 msec) were maintained at the inner edge of the SAP grid.

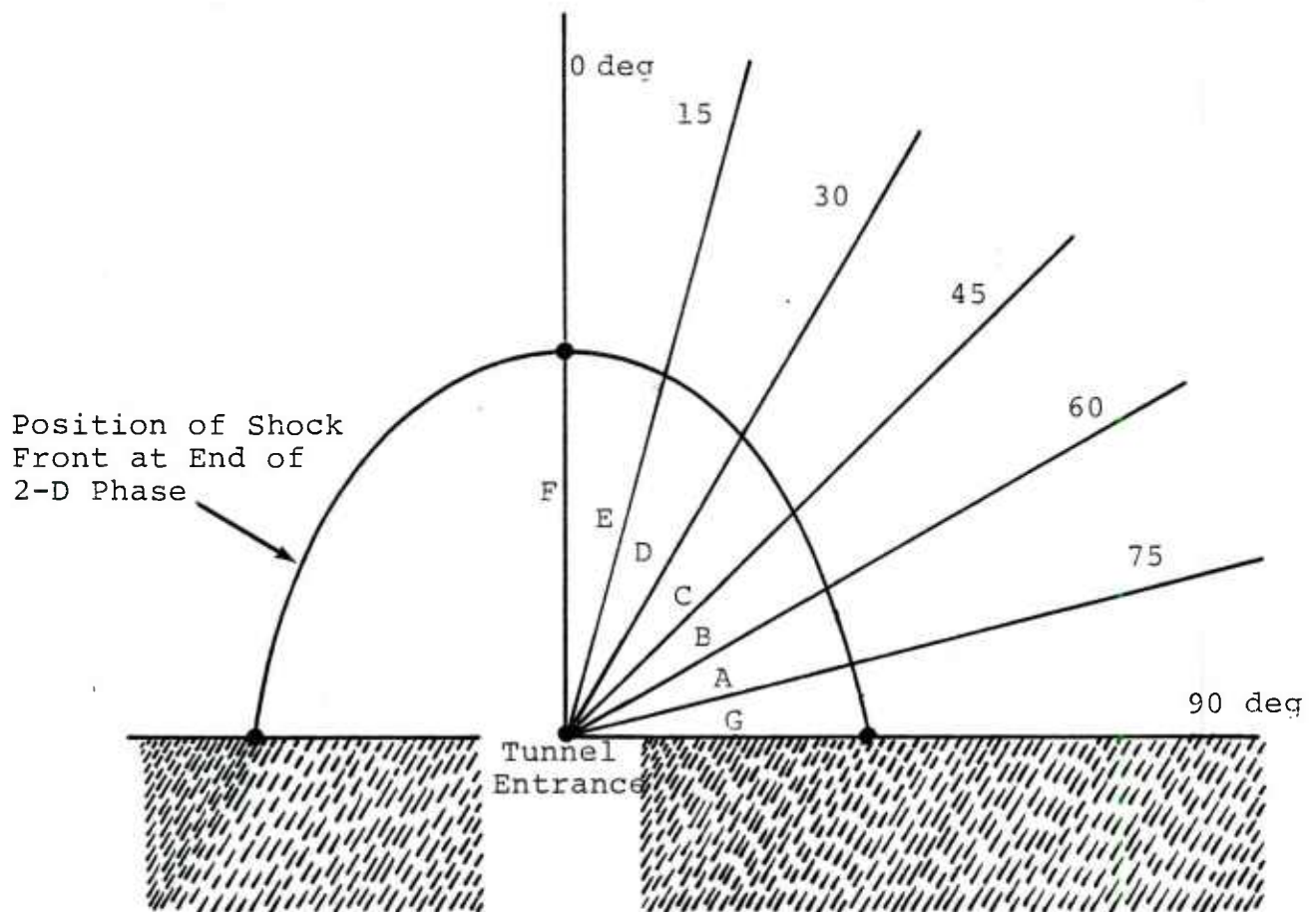


Figure 29. Calculational Configuration Showing Lines Along Which One-Dimensional Calculations Were Performed

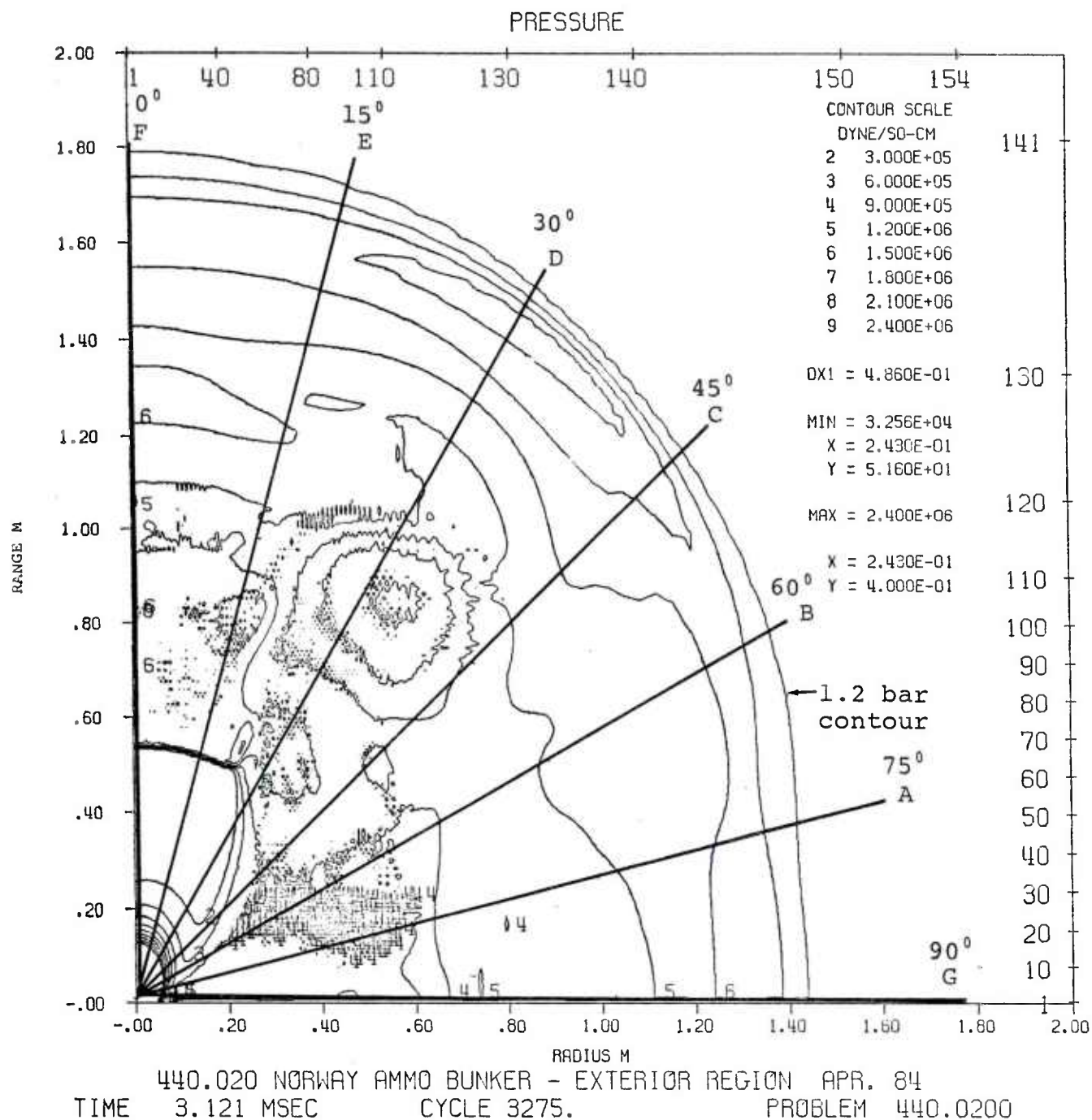
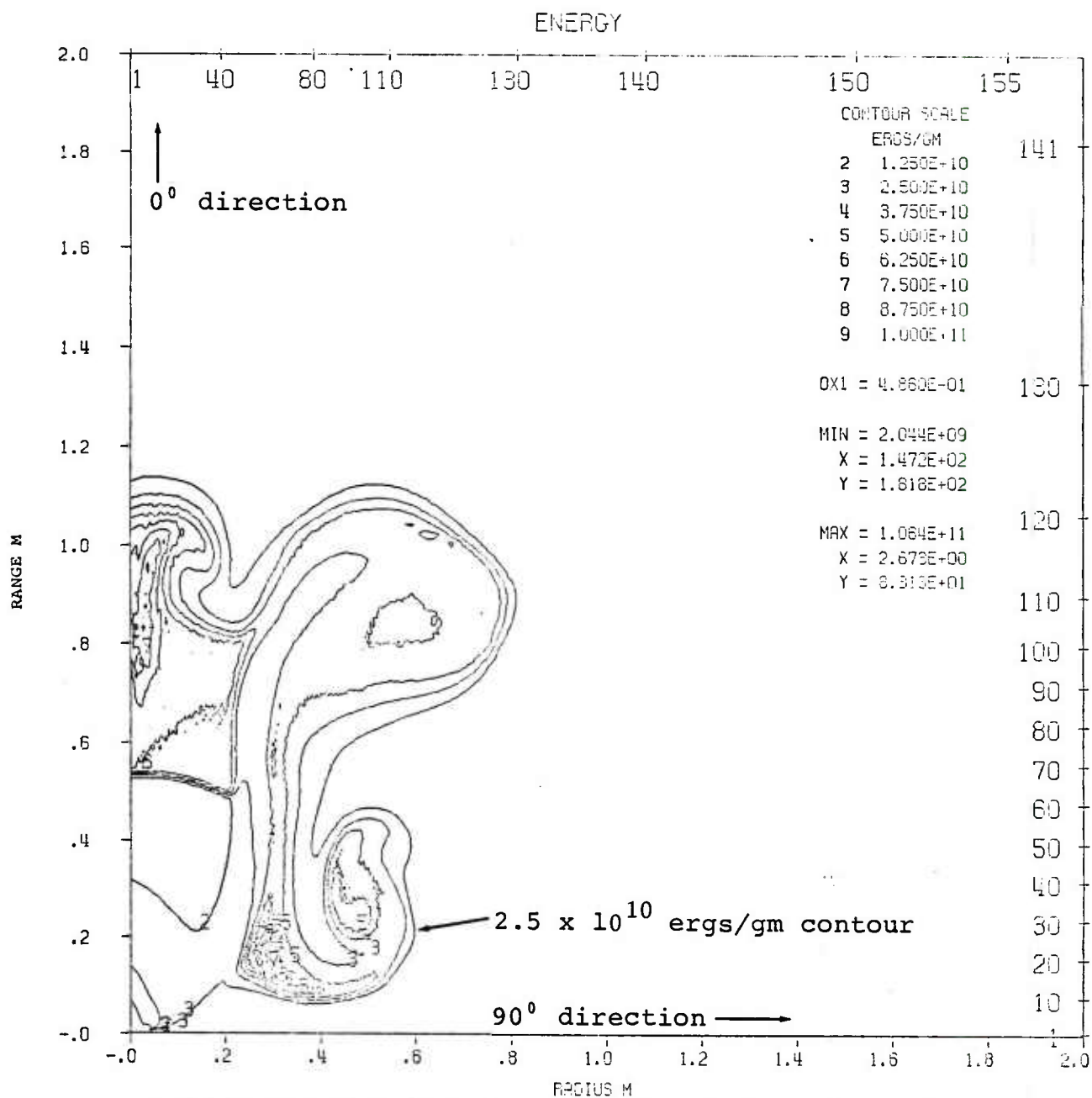


Figure 30. Pressure Contours at 3.1 msec Used for Initiation of Phase 3



440.020 NORWAY AMMO BUNKER - EXTERIOR REGION APR. 84  
 TIME 3.121 MSEC CYCLE 3275. PROBLEM 440.0200

Figure 31. Energy Contours at 3.1 msec Used for Initiation of Phase 3

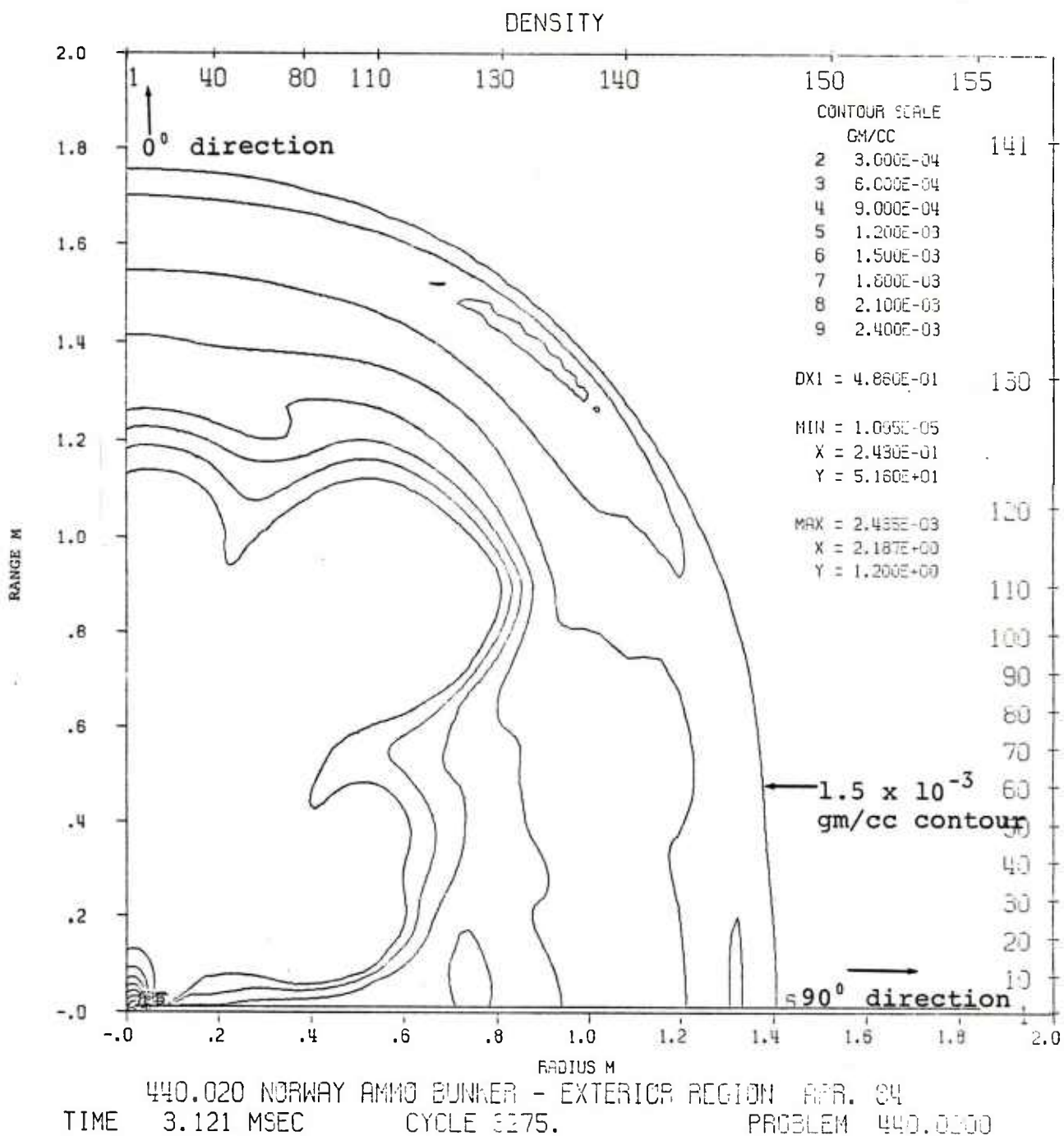


Figure 32. Density Contours at 3.1 msec Used for Initiation of Phase 3



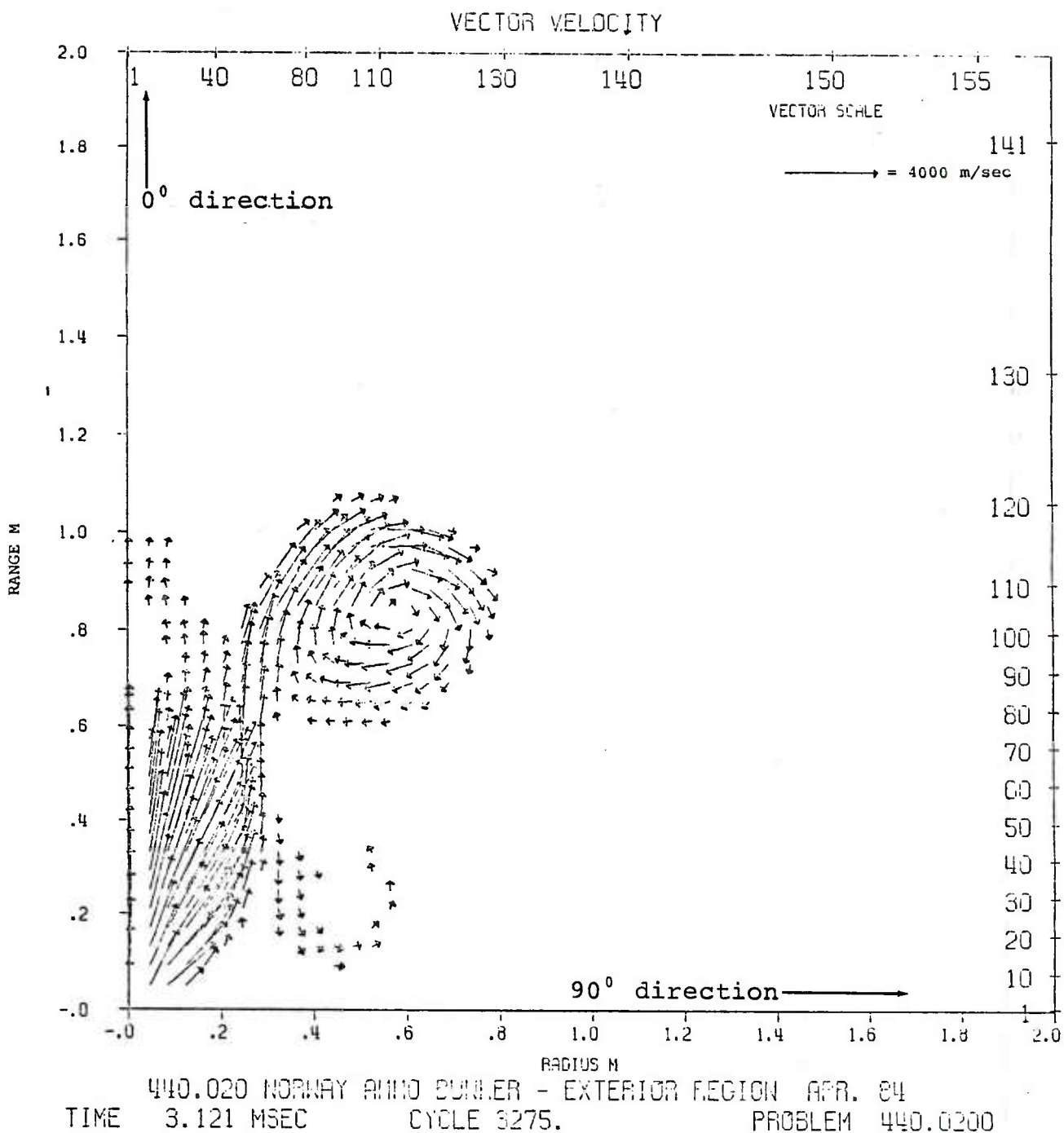


Figure 33. Flow Velocity Vector Plot at 3.1 msec Used for Initiation of Phase 3

Figures 34 through 40 are overpressure versus range plots, one for each of the seven SAP calculations, at the final time for that calculation. These range plots provided the waveforms from which inputs for NLAWS, the acoustic wave propagation code used in Phase 4, were defined.





# OVERPRESSURE

NORWAY AMMO BUNKER-EXTERIOR LINE G

90°

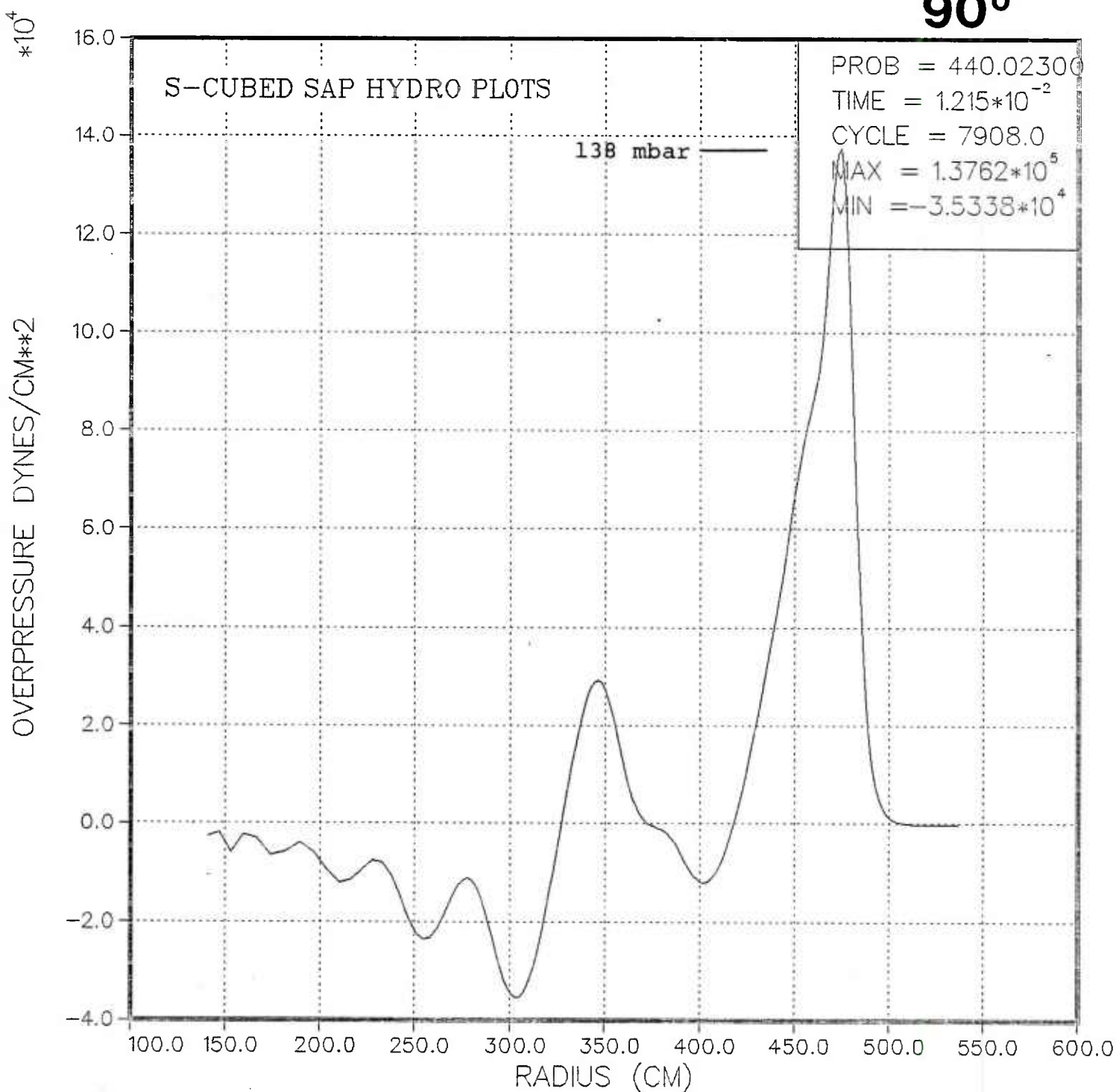


Figure 34. Overpressure versus Range Plot Along 90°  
Line at 12.15 msec



# OVERPRESSURE

NORWAY AMMO BUNKER-EXTERIOR LINE A

**75°**

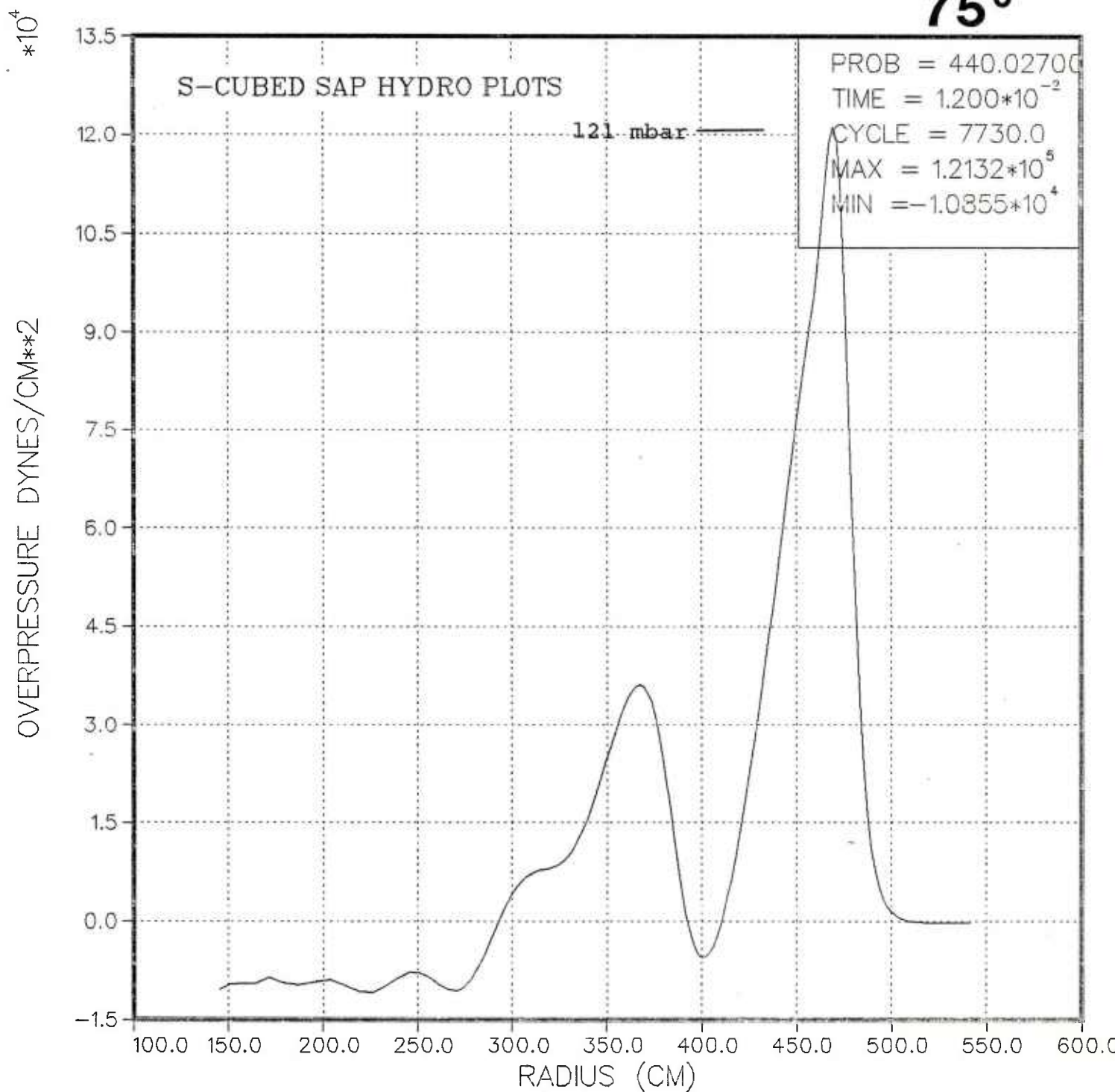


Figure 35. Overpressure versus Range Plot Along 75° Line at 12.00 msec



# OVERPRESSURE

NORWAY AMMO BUNKER—EXTERIOR LINE B

**60°**

\*10<sup>4</sup>

OVERPRESSURE DYNES/CM\*\*2

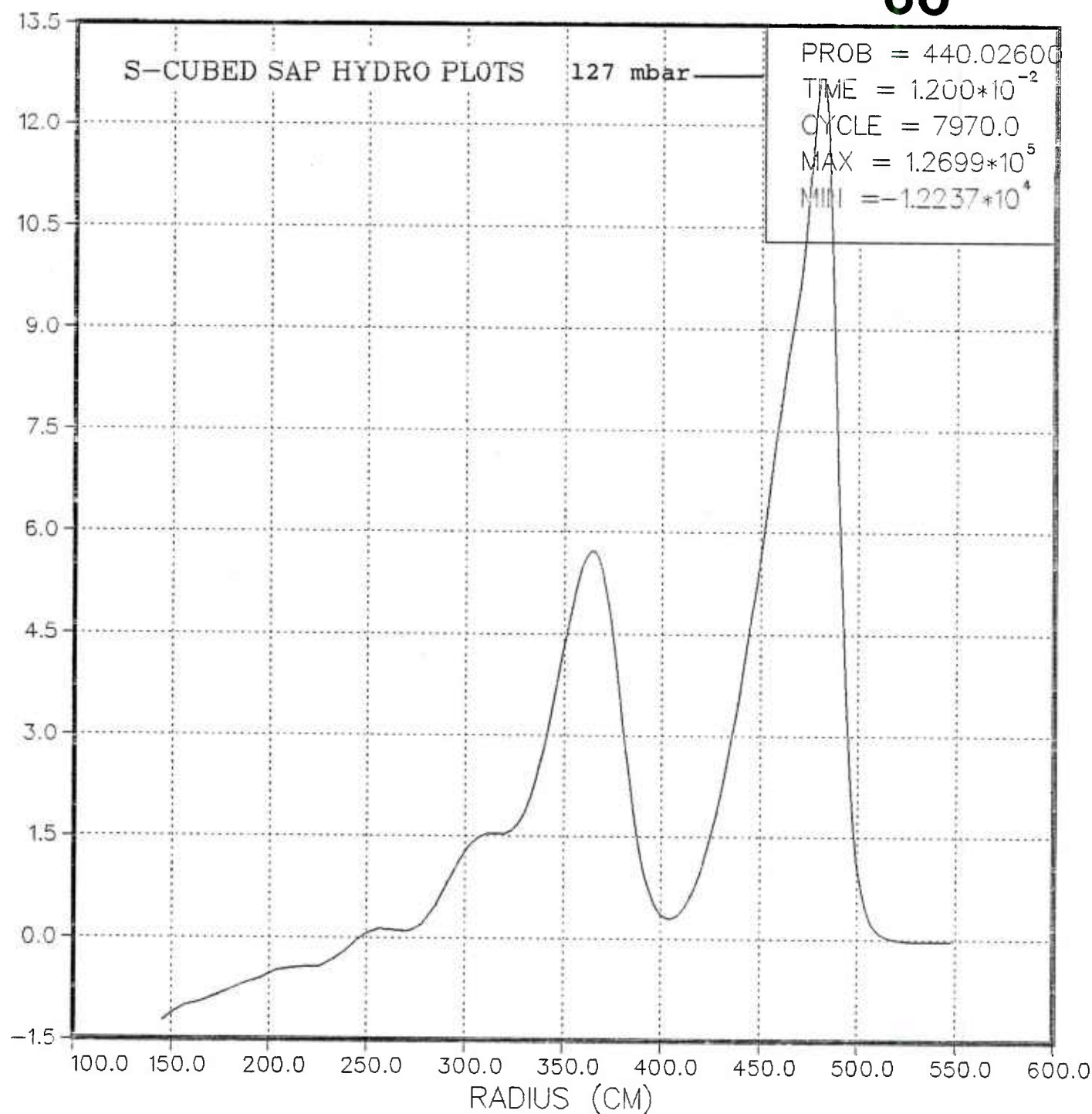


Figure 36. Overpressure versus Range Plot Along 60° Line at 12.00 msec



# OVERPRESSURE

NORWAY AMMO BUNKER-EXTERIOR LINE C

**45°**

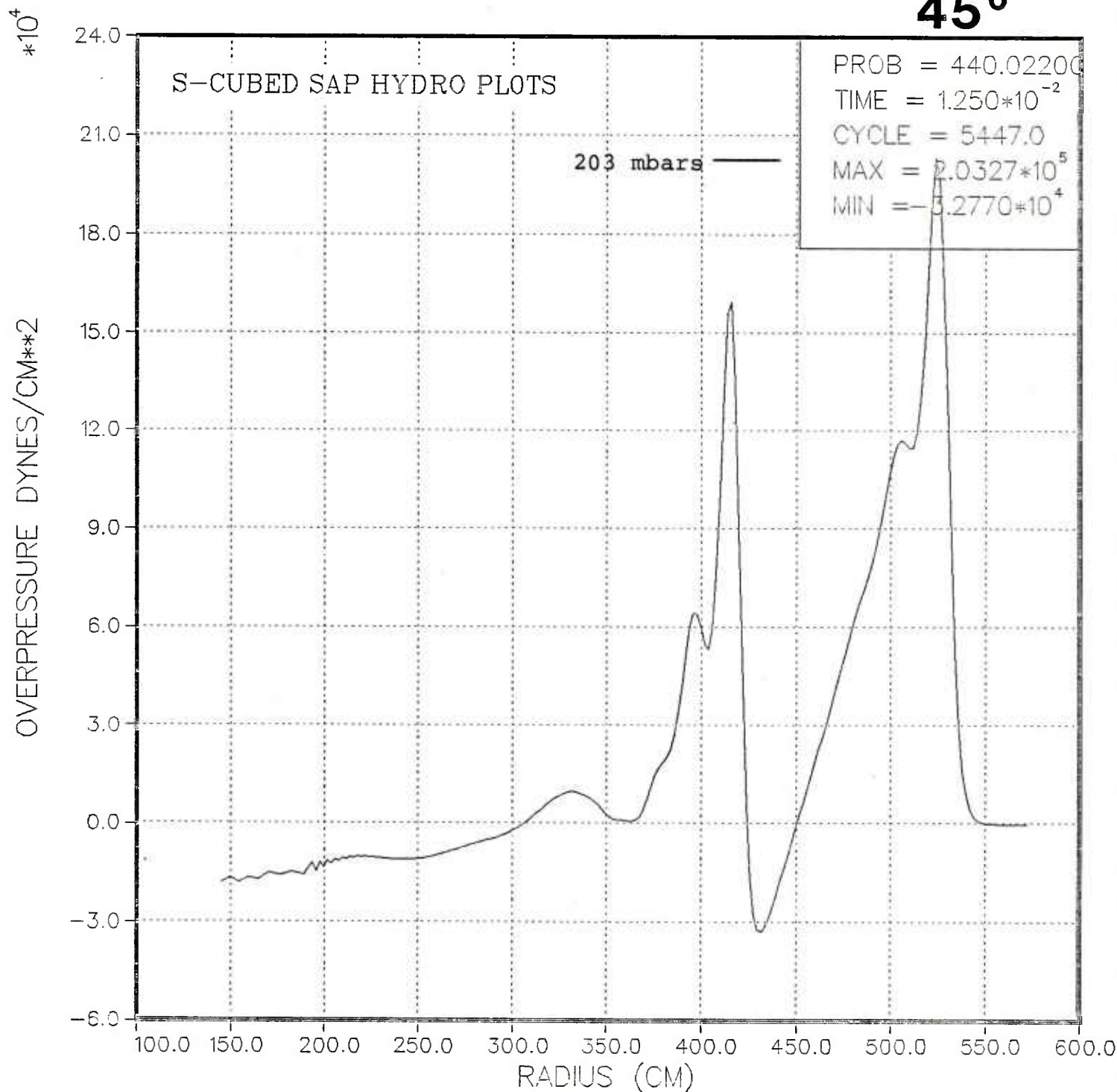


Figure 37. Overpressure versus Range Plot Along 45° Line at 12.50 msec





# OVERPRESSURE

NORWAY AMMO BUNKER-EXTERIOR LINE D

**30°**

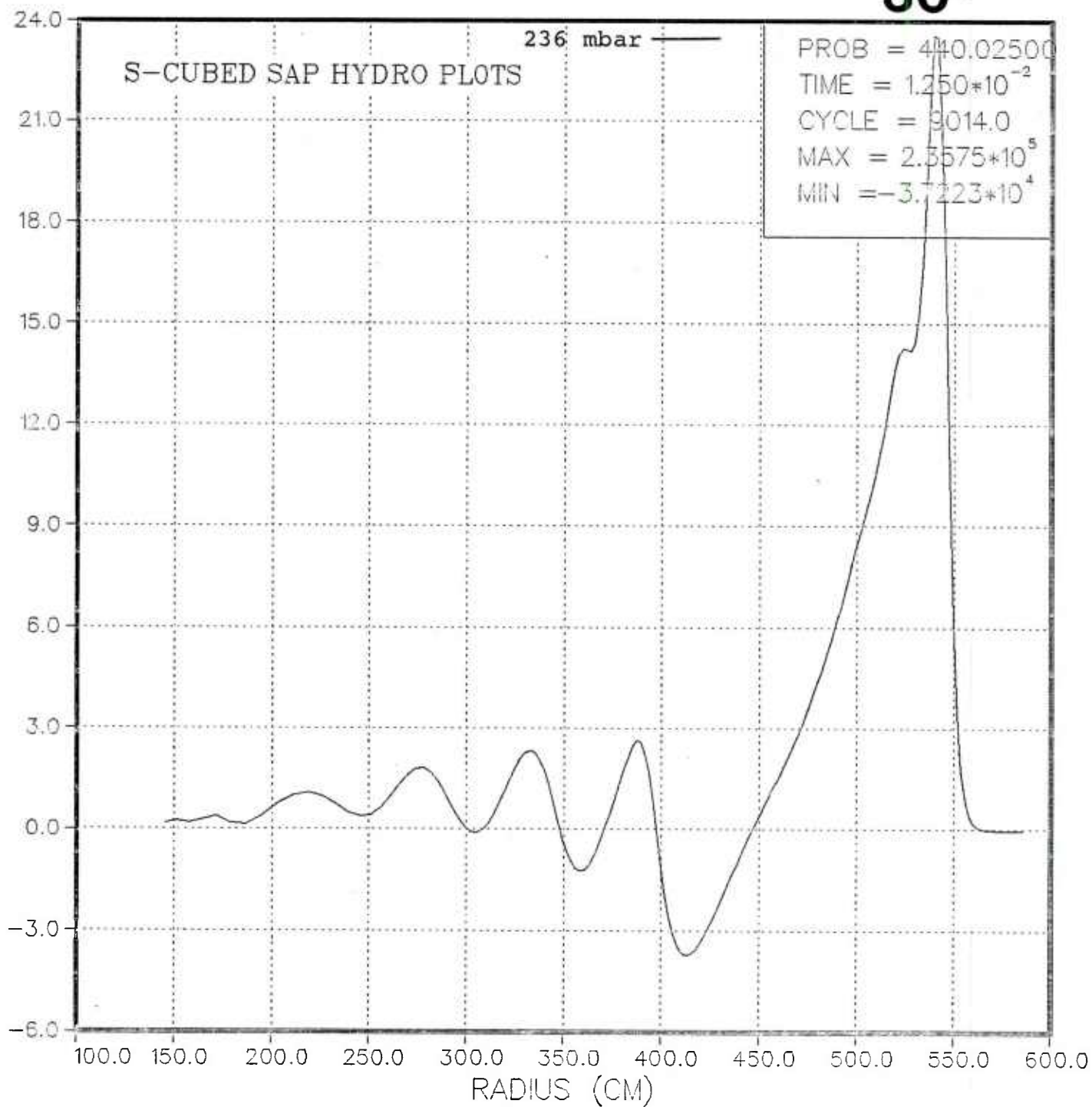


Figure 38. Overpressure versus Range Plot Along 30° Line at 12.50 msec



# OVERPRESSURE

NORWAY AMMO BUNKER-EXTERIOR LINE E

15°

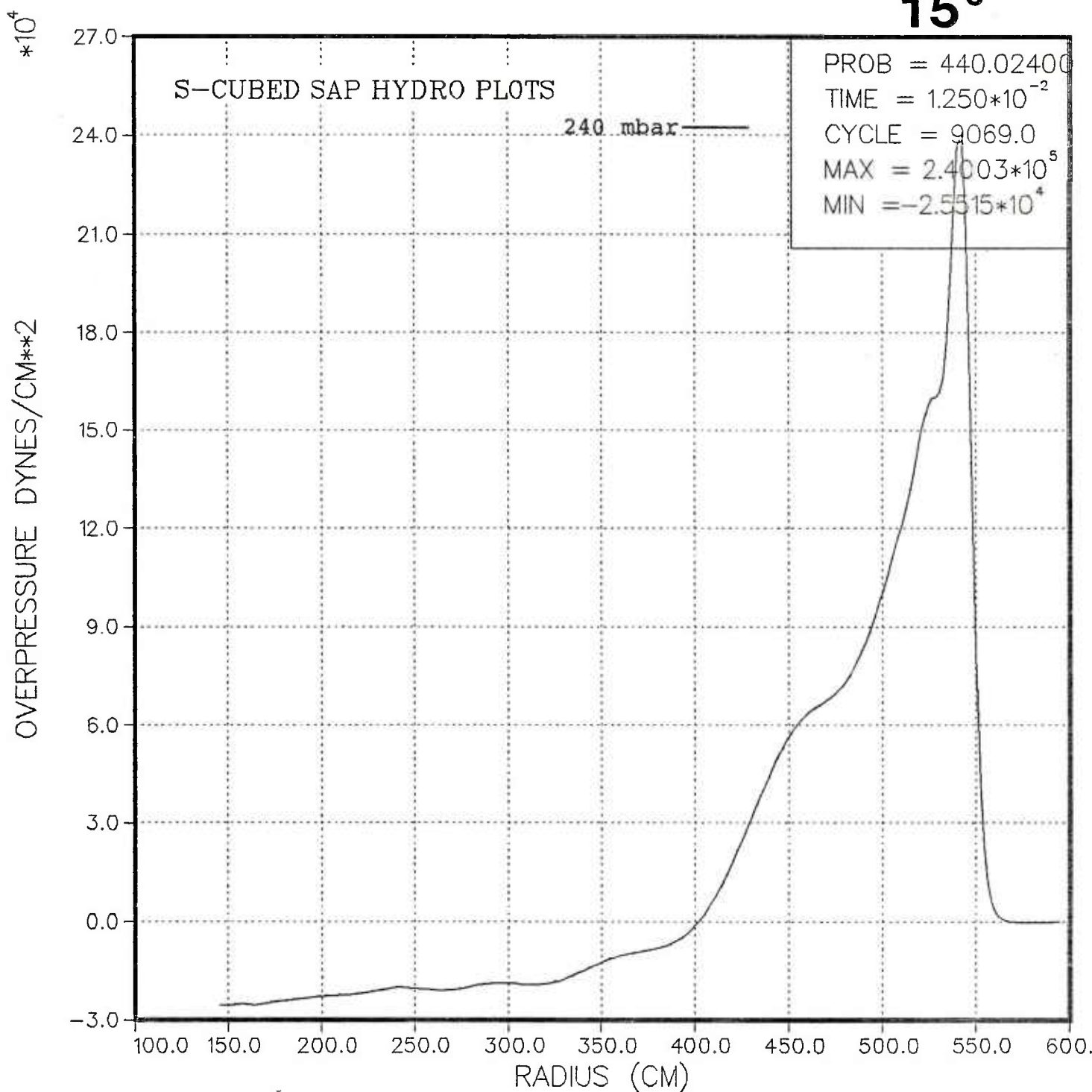


Figure 39. Overpressure versus Range Plot Along 15° Line at 12.50 msec



# OVERPRESSURE

NORWAY AMMO BUNKER-EXTERIOR LINE F

0°

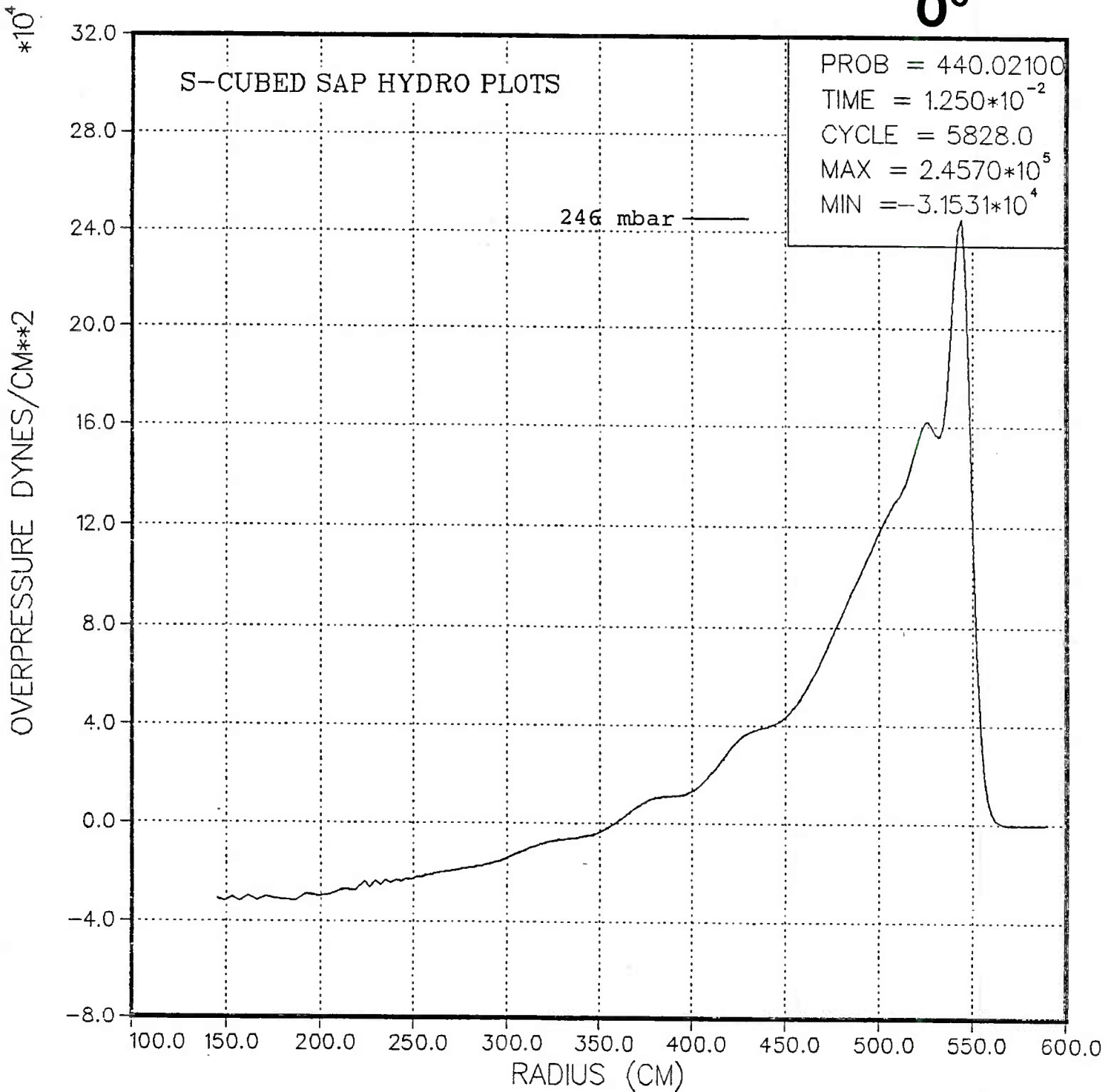


Figure 40. Overpressure versus Range Plot Along 0° Line at 12.50 msec

## V. PHASE 4: NONLINEAR ACOUSTIC WAVE SOLUTION (NLAWS)

NLAWS is a code which treats the airblast waveform as an acoustic wave. The code assumes an ideal triangular waveform input with an infinitely sharp rise to a positive overpressure and then a monotonic decay to zero. The triangular wave is then propagated acoustically until it has attenuated to the desired level. NLAWS was written at the Air Force Weapons Laboratory and is used to find the peak overpressure and velocity at ranges below approximately 280 mbar (4 psi).

The NLAWS program was run for each of the one-dimensional calculations, beginning at the last time from the SAP calculations of Phase 3. The objective was to determine a range at which the peak overpressure would have attenuated to 50 mbar. Because the input waveform for NLAWS must be triangular, waveforms from the SAP one-dimensional calculations had to be modified. This was done in the following manner. First, a vertical line was drawn through the mid-point of the first rise on the SAP waveform. In Figure 41, this line is designated "LINE 1". Second, a representative slope was chosen on the falling portion on the wave, and a line was drawn tangent to the sloping portion (illustrated by "LINE 2" in Figure 41). These two lines defined a peak overpressure and a positive phase duration for input to NLAWS. Because there was some uncertainty about the choice of the tangent line, a second line (LINE 3) was chosen and a second NLAWS calculation was performed. Choosing the input waveform in this manner eliminates numerical shock-front smearing and any numerical overshoot from the hydrocode results. The two different NLAWS calculations provide an estimate of the accuracy of the results.





# OVERPRESSURE

NORWAY AMMO BUNKER-EXTERIOR LINE F

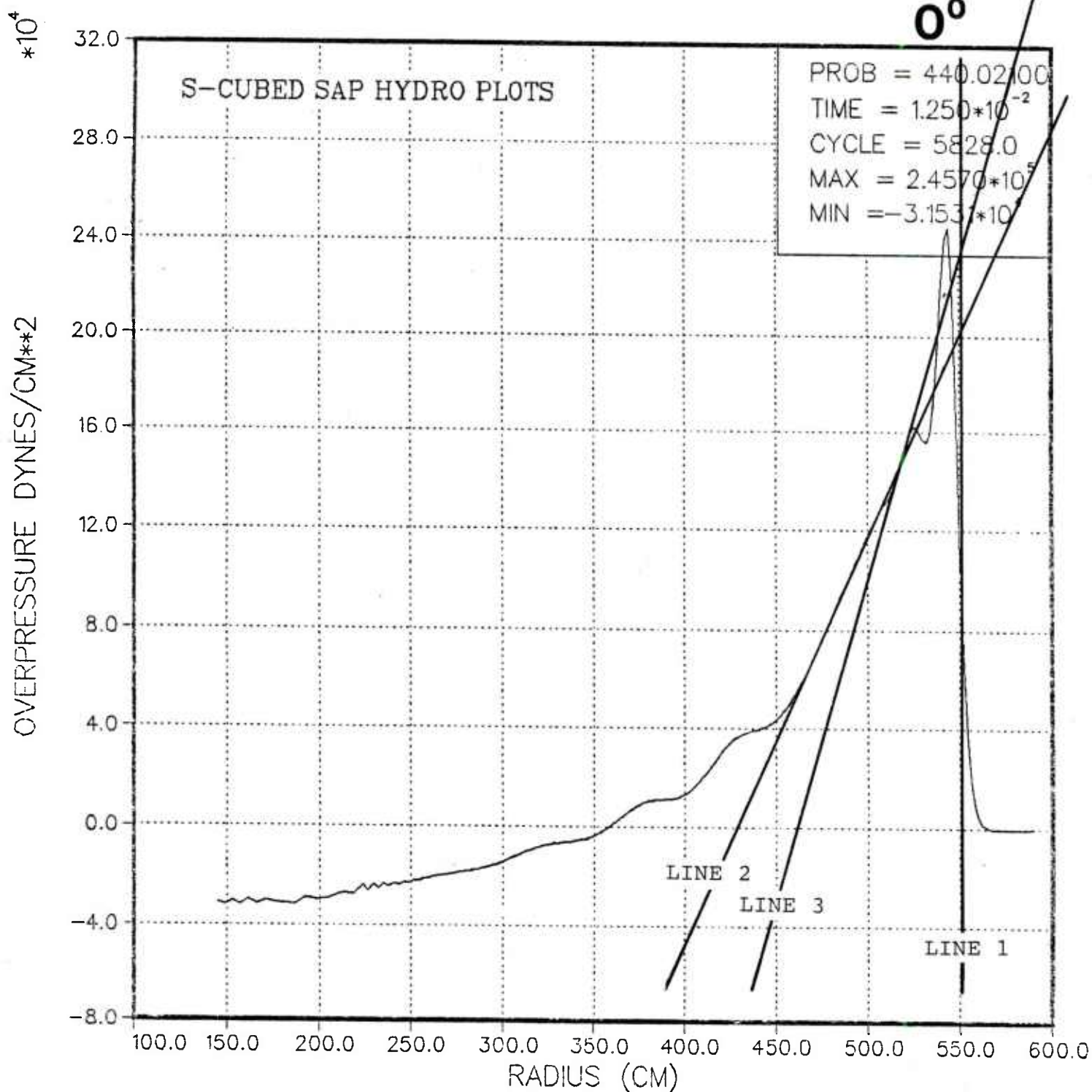


Figure 41. Overpressure vs. Range Plot Showing Method of Determining Triangular Wave Input for NLWS

The procedure described previously was applied to each of the seven waveforms from the SAP calculations given in the last section. In cases such as that for the 45 deg line (Figure 37), in which waveform consisted of two distinct pulses, only the first (and largest) was used. Under acoustic conditions, all parts of a wave propagate at the same speed, thus there is no overtaking of the front-running portions by those following.

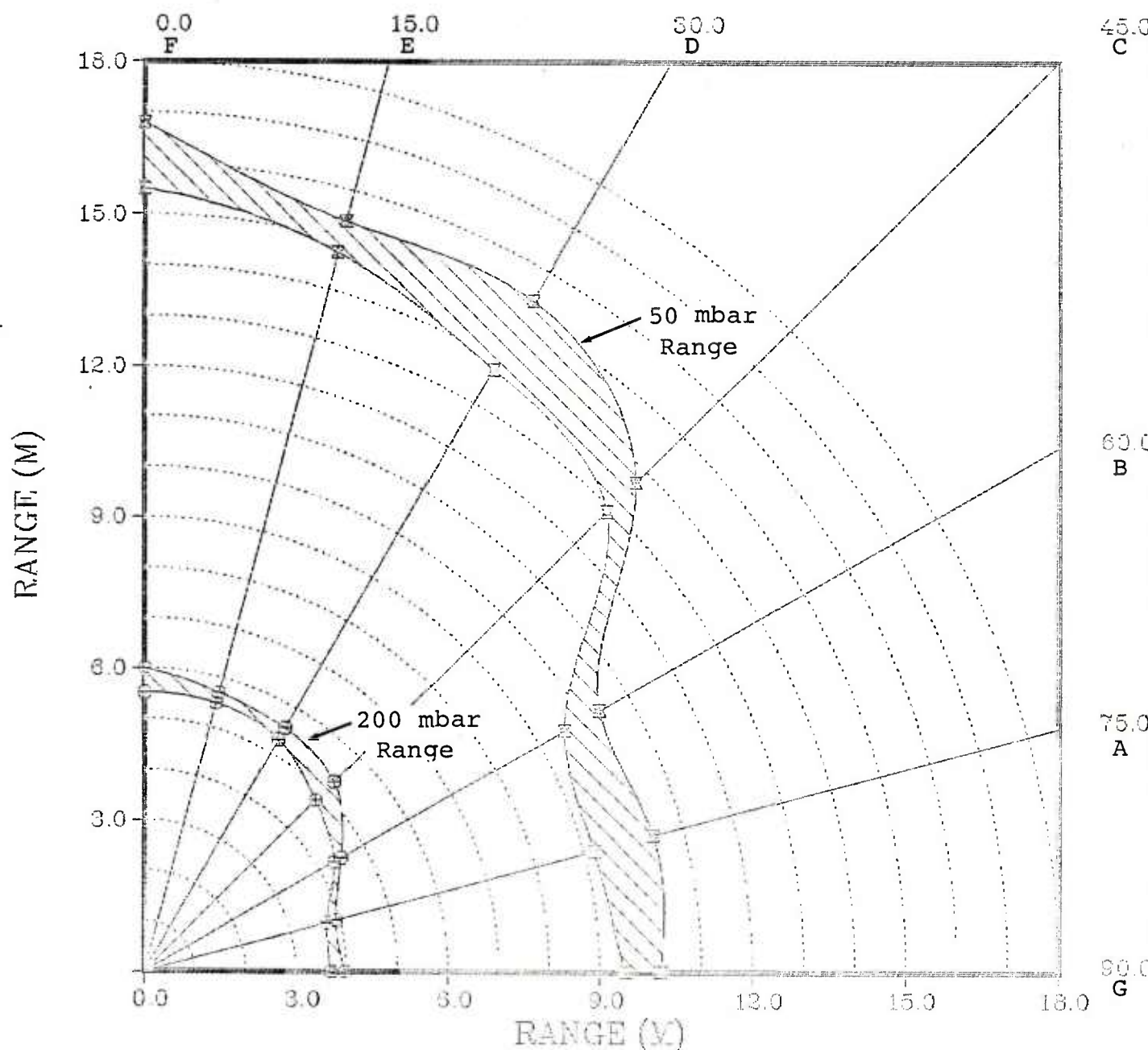
## VI. CONCLUSIONS

The peak-overpressure versus range listings generated by NLAWS as described in the previous section were interpolated as necessary to determine the range at which this peak falls below 50-mbars. Because two sets of input conditions were defined, a spread in range was obtained at each angle. The results are shown in Figure 42 (outer curve). As can be seen, for positions directly in front of the tunnel entrance (0 deg), a distance of 17 meters is required to assure that the peak overpressure experienced will be less than 50 mbars. For off-axis positions, 16 meters is sufficient at 15 and 30 deg and 14 meters at 45 deg. At angles of 60 deg or greater, only 11 meters is required. For the full-scale situation of interest, in which 200,000 kgm of explosive are detonated, all distances would be scaled up by a factor of 100.

The inner curve in Figure 42 defines the 200-mbar peak overpressure distances. This curve was determined in exactly the same way as the 50-mbar curve, except that in this case the results were taken from the early part of the NLAWS run or, at several of the angles, directly from the SAP results.



# NORWAY AMMO BUNKER-EXTERIOR



## OVERPRESSURE CONTOURS

Figure 42. Ranges for 50 and 200 mbar Peak Overpressures as Functions of Angle